Multiple post-Caledonian exhumation episodes across northwest Scotland revealed by apatite fission track analysis

Simon P. Holford[1], Paul F. Green[2], Richard R. Hillis[1], John R. Underhill[3], Martyn S. Stoker[4] & Ian R. Duddy[2]

[1]Australian School of Petroleum, Centre for Tectonics, Resources and Exploration (TRaX), University of Adelaide, SA 5005, Australia (simon.holford@adelaide.edu.au)

[2]Geotrack International Pty Ltd, 37 Melville Road, Brunswick West, Victoria 3055, Australia

[3]School of Geosciences, The University of Edinburgh, Grant Institute of Earth Science, The King's Buildings, West Mains Road, Edinburgh EH9 3JW, United Kingdom

[4]British Geological Survey, Murchison House, West Mains Road, Edinburgh EH9 3LA, United Kingdom

Abstract

The post Caledonian exhumation history of northwest Scotland is a controversial issue, with some studies advocating largely continual emergence while others suggest dominantly early Palaeogene plume-driven exhumation. AFTA data in samples of Precambrian basement and Permian-Cretaceous sediments from onshore and onshore reveal multiple phases of post-Caledonian cooling, viz: Triassic (beginning 245-225 Ma), Cretaceous (140-130 Ma; 110-90 Ma) and Cenozoic (65-60 Ma; 40-25 Ma; 15-10 Ma), all of which are interpreted at least in part as recording exhumation. Basement and sedimentary cover rocks display similar thermal histories, emphasising the regional nature of these episodes and implying that sedimentary outliers represent the remnants of previously more extensive sequences. Significant thicknesses of Jurassic rocks may once have covered northwest Scotland. Palaeocene palaeothermal effects are most pronounced in the vicinity of igneous centres, probably reflecting combined effects of heating by elevated heat flow, deeper burial and hydrothermal activity. Most of the region underwent km-scale Neogene exhumation. Contrary to the

common assumption of monotonic cooling and denudation histories, integration of geological evidence with AFTA data defines an episodic thermal history involving repeated cycles of burial and exhumation. We suggest that onshore passive margins and continental interiors may also best be characterised by similar histories.

Abstract

The origin and development of the high topography bordering the Atlantic margin of NW Europe has long been the subject of debate (Geike, 1901; George, 1966; Doré et al., 2002). The mountains of Scotland and western Scandinavia are characterized by rugged topography and elevations that exceed 1.3 km and 2.4 km respectively and largely comprise rocks that were formed and/or deformed during the Caledonian Orogeny. Numerous lines of evidence indicate that the present-day topography of both regions was initiated by tectonic uplift that began during the Cenozoic or late Mesozoic and which also affected peripheral sedimentary basins (Doré et al., 2002). These include; the transition from deposition of shallow-marine carbonates in the late Cretaceous to rejuvenated clastic sedimentation in the early Palaeogene (Doré et al., 2002)); the easterly tilt of Britain (Brodie & White, 1994); identification of Palaeocene, Eocene and Pliocene-Pleistocene prograding and locally heavily incised shelf-slope wedges of clastic sediments offshore Scotland and Norway (Stoker et al., 1993, 2010; Underhill, 2001); apatite fission track, vitrinite reflectance and sonic velocity data which record deeper burial of Cenozoic-Mesozoic sediments and Palaeozoic and older basement rocks along the Atlantic margin prior to their uplift and erosion (Japsen et al., 2007; Hillis et al., 2008); and, geomorphological evidence for elevation of low-relief erosion surfaces and

landscape elements formed at or near sea level during the Mesozoic and Palaeogene and subsequently uplifted (Japsen et al., 2002).

Despite this evidence for tectonically driven uplift of the Atlantic margin during the late Mesozoic and Cenozoic, it has been recently proposed (Nielsen et al., 2009) that the present-day topography of western Scandinavia and the Scottish Highlands represents remnant topography from the Caledonian Orogeny that survived post-orogenic extensional collapse and erosion. Nielsen et al. (2009) suggest that many of the observations listed above that have been used to argue for Cenozoic tectonic uplift can instead be interpreted in terms of protracted exhumation maintained by climatically-controlled erosion rates. This hypothesis implies that the Scottish Highlands and western Scandinavia have been positive topographic features for the past ~400 million years, experiencing no significant burial and receiving little or no Upper Palaeozoic-Cenozoic sediments (cf. Macdonald et al., 2007).

Recent apatite fission track and (U-Th)/He data from basement samples in the Scottish Highlands have been interpreted in terms of thermal histories dominated by continuous, monotonic cooling and exhumation over the past ~400 Myr (Persano et al., 2007) and thus support the idea of continuous, post-Caledonian emergence (cf. Watson, 1985). Such monotonic cooling of basement rocks is inconsistent with the local geological record however, because outliers of Devonian, Carboniferous, Permian-Triassic, Jurassic and Cretaceous sediments overlying Neoproterozoic basement (e.g. Moine Supergroup, Torridonian) are found along the coast of northwest Scotland (Fig. 1). In addition, thick sequences of mainly Triassic-Jurassic age sediments are preserved in offshore basins of the Malin-Hebrides sea area (Fyfe et al., 1993), whilst the overstep of Old Red Sandstone onto late Caledonian granites indicates that Caledonian topography had largely been worn down by rapid uplift and erosion during the early Devonian (Hall, 1991).

Conversely, other workers have claimed that Scotland has experienced post-Caledonian tectonically-driven uplift that was dominantly early Palaeogene in age and driven by processes associated with the Iceland mantle plume, such as igneous underplating or convectively-supported dynamic uplift (White & Lovell, 1997; Jones et al., 2002; Shaw Champion et al., 2008). However, recent fission-track studies from the southern British Isles have revealed a more complex Mesozoic-Cenozoic uplift history, with major phases of km-scale uplift and exhumation occurring during the early Cretaceous and Neogene in addition to the early Palaeogene (Holford et al., 2005; Hillis et al., 2008; Holford et al., 2009a, b, c).

The aim of this study is to test these different models for the post-Caledonian tectonic evolution of northwest Scotland using a new apatite fission-track analysis (AFTA) database comprising onshore and offshore samples from basement (i.e. Lower Palaeozoic and older) and from the Permian-Cretaceous sediments deposited in overlying sedimentary basins. The offshore database includes samples collected over a range of depths from exploration wells located in the Sea of the Hebrides (134/5-1) and West Orkney (202/19-1) basins that provide direct constraints on palaeogeothermal gradients and allow estimates of amounts of missing section removed during exhumation. Thermal history solutions extracted from our data show consistency between samples from basement and cover sequences and show that the Mesozoic sediments deposited around northwest Scotland have been heated to temperatures exceeding 100°C during burial by additional sedimentary sequences. The preserved sediments are thus interpreted as remnants of deposits that were originally far more extensive, raising the possibility that the Highlands were buried beneath a Mesozoic sedimentary cover.

The additional sedimentary sequences were removed during a series of Cretaceous-Cenozoic exhumation episodes, whose timing is constrained by both AFTA data and unconformities that separate the sedimentary units. Our results indicate that interpretations involving continual post-Caledonian emergence cannot be sustained, and that the post-400 Ma history of northwest Scotland has been characterised by repeated cycles of sedimentation and exhumation, suggesting that post-Caledonian events are largely responsible for the physiography of northwest Scotland.

Post-Caledonian geological history of northwest Scotland

The Caledonian orogeny in northwest Scotland culminated during the Lower Devonian (Fyfe et al., 1993). The onset of extensional tectonics in the Middle Devonian facilitated the collapse of the Caledonian mountain belt (Stoker et al., 1993). Thick sequences of Old Red Sandstone (ORS) continental sediments and lavas occur within the Midland Valley, southeast of the Highland Boundary Fault (Fyfe et al., 1993) and large areas of Devonian sedimentary rocks in northeast Scotland are remnants of the originally more extensive Orcadian Basin (Hillier and Marshall, 1992) (Fig. 1). Limited ORS siliciclastic and volcanic outcrops of Lower Devonian age around Oban and in the Firth of Lorne are interpreted to be the preserved remnants of a formerly more extensive ORS cover (Fyfe et al., 1993). Carboniferous rocks are of limited exposure in the Scottish Highlands with the exception of ~100 m of Carboniferous sandstone preserved on Morvern (Fyfe et al., 1993), although considerably thicker sequences (up to 3 km) of marine and nonmarine Carboniferous sediments are preserved within the Midland Valley Basin (Underhill et al., 2008).

Permian-Triassic continental redbeds are widely distributed in the basins offshore northwest Scotland (Fig. 1), reaching thicknesses of ~3 km in the North Minch Basin (Fyfe et al., 1993).

Upper Triassic sediments are exposed on Skye, Ardnamurchan, Mull, Morvern, Applecross, Gruinard Bay and on northeast Lewis where ~1.2 km of Permian-Triassic sandstones and conglomerates rest with unconformable or faulted contact against Lewisian gneisses (Fyfe et al., 1993). These basins also contain thick sequences of marine and nonmarine Jurassic deposits, and there are onshore outcrops along the northwestern coast of Scotland and on Skye and Raasay where the Jurassic succession reaches 450 m (Fyfe et al., 1993). Based on detailed subsidence analyses of preserved Triassic-Jurassic rocks in the Inner Hebrides, Morton (1987) proposed that the initial phase of crustal stretching responsible for the Hebridean basin system commenced during the late Triassic (~210 Ma).

Cretaceous rocks are less widely distributed (Fig. 1), but this is considered to be due Cenozoic uplift and erosion rather than non-deposition (Hallam, 1983). Upper Cretaceous sediments are preserved on Morvern, including glauconitic and pure silica sandstones overlain by silicified Chalk (Fyfe et al., 1993). The Cretaceous rocks on Morvern rest unconformably on Triassic-Jurassic strata, implying an intervening period of erosion, probably during the early Cretaceous (Hallam, 1983). There are minor outcrops of Upper Cretaceous strata on Skye, Mull, Eigg and Arran but no rocks of this age have been proven immediately offshore (Fyfe et al., 1993).

Widespread volcanicity accompanied continental breakup between Greenland and northwest Europe in the late Palaeocene-early Eocene along the North Atlantic margins (Emeleus and Bell, 2005). Most volcanicity in the British Isles was concentrated in northwest Scotland, with major igneous centres at Mull, Ardnamurchan, Rum and Skye (Emeleus and Bell, 2005). This igneous activity has been attributed to the proto-Iceland mantle plume, and petrological data suggest that a significant proportion (up to 70%) of the melt generated around the British

Isles was trapped at depth, leading to underplating of the lower crust, which in turn would have resulted in surface uplift (Jones et al., 2002). However, the depth to the seismic reflection Moho beneath northwest Scotland is low compared to southeast Scotland (varying from 25 to 29 km beneath basins and basement) (Chadwick and Pharaoh, 1998) and is inconsistent with the crust having been significantly thickened by igneous material.

Climatic deterioration during the Quaternary profoundly affected the landscape of the Scottish Highlands, with decreasing temperatures permitting the growth of glaciers on uplifted terrain which in turn promoted widespread erosion and deposition of glacial glaciomarine sediments offshore northwest Scotland (Stoker et al., 1993).

AFTA methodology and database

The methodological and analytical aspects of AFTA are well established (e.g. Green et al., 2002). AFTA utilizes the radiation damage trails (fission tracks) created by spontaneous fission of ^{238}U within the crystal lattice of apatite, which is a common detrital mineral in most sandstone and occurs as an accessory phase in plutonic and high grade metamorphic rocks. By counting the number tracks in a polished and etched grain surface and measuring the uranium content, a fission track age can be calculated, which in the absence of other factors would provide a direct measure of the time over which tracks have accumulated. Fission track lengths form within a narrow range (~16 μm), but are progressively shortened as radiation damage is repaired at a rate that increases with temperature (annealing). Shortening leads to a reduction in the number of tracks that can intersect a polished surface, and above 110°C all damage is repaired and no tracks are preserved. A measured fission track age thus represents a balance between production of tracks and loss by annealing, and must be assessed in tandem with track length data.

We present AFTA data from 78 samples collected from onshore and offshore northwest Scotland (Fig. 1, Table 1). Our dataset includes 42 samples from onshore outcrops, 21 samples from British Geological Survey (BGS) offshore shallow boreholes and drill cores, and 15 samples from two wells (202/19-1 in the West Orkney Basin (WOB) and 134/5-1 in the Sea of Hebrides Basin (SOHB)). The samples cover a broad range of stratigraphic levels, from Proterozoic (Torridonian and Moine) and Archean (Lewisian) basement to Phanerozoic sedimentary cover rocks of Permian, Triassic, Jurassic and Cretaceous age. Data quality is generally excellent, with the majority of samples yielding 20 or more single grain ages and many samples yielding 100 track lengths (Table 1).

The majority of measured fission track ages are younger than the respective stratigraphic ages (Table 1). Overall there is a consistent trend between fission track age and mean track length, with most fission track ages in the range of 150-300 Ma regardless of the depositional or metamorphic age of the host rock, and mean track lengths (MTLs) in the range 11-13 µm (Fig. 2). Samples from Skye yield much younger fission track ages between 50 and 70 Ma, with mean track lengths around ~13-14 µm. The main trend in Fig. 2 is very different from the simple "boomerang trend" shown by samples that have undergone a single heating event in which different samples have undergone varying degrees of resetting (Green, 1986), and suggests that the region has undergone a relatively complex history involving a series of resetting events.

With the exception of one sample (GC503-151), the fission track ages of all samples from northwest Scotland are younger than 400 Ma and the overwhelming majority are younger than 300 Ma i.e. at least 100 Myr younger than the latest stages of Caledonian Orogeny. This immediately indicates that almost all basement and early Palaeozoic samples reached palaeotemperatures sufficient to produce severe age reduction (i.e. ~100°C or above) during post-Caledonian events. Moreover, Proterozoic and Achaean basement samples tend to yield similar fission track ages and length distributions to nearby Phanerozoic cover samples (Table 1 and Fig. 2), suggesting that basement and cover sequences in northwest Scotland have undergone similar thermal histories.

Thermal history interpretation of AFTA data

Basic principles

Extraction of thermal history information from AFTA data begins with construction of a Default Thermal History (DTH), derived from the burial history defined by the preserved sedimentary section and the present-day thermal gradient. For a sedimentary rock, this is the history which would apply if the sample has never been any hotter than the present-day temperature at any time since deposition. For basement samples, a similar approach can be adopted using the age of the oldest overlying sedimentary units, which in this study we have assumed to be Devonian if no sedimentary units are present. If the DTH can explain the AFTA data, then it is not possible to extract further thermal history information. If the AFTA data show a greater degree of annealing (i.e. fission track age and/or track length reduction) than expected from the DTH, then the sample must have been hotter in the past and information on the magnitude and timing of heating and cooling events can be extracted from the data. All samples analysed in this study show a greater degree of annealing (i.e. fission track age and/or length reduction) than that expected from the DTH , and have therefore been much hotter in the past.

To extract thermal history information from AFTA data, we use a kinetic model that makes full quantitative allowance for the effects of Cl content on fission-track annealing rates

(Green et al., 2002). Because maximum palaeotemperatures are the key factor that dominates AFTA data, this technique reveals little information on the thermal history prior to the onset of cooling. Therefore, we do not attempt to constrain the entire thermal history of each sample but focus on the key aspects of the thermal history that control the fission track age and length distribution i.e. the maximum palaeotemperature of each sample, and the time at which cooling from that palaeotemperature began.

By modelling expected AFTA parameters resulting from a range of possible thermal histories, we use maximum likelihood theory similar to that described by Gallagher (1995) to define the range of values of maximum palaeotemperature and the onset of cooling giving predictions which match the measured data within 95% confidence limits. Palaeotemperature estimates derived using this approach usually have an absolute uncertainty of better than ±10°C. Many of the samples analysed in this study require at least two episodes of heating and cooling to explain all facets of the data. AFTA can provide constraints on two episodes provided the magnitude and timing of the palaeothermal maximum and the subsequent (lower) peak palaeotemperature are sufficiently separated. In some cases (e.g. Turner et al., 2008) it is possible to resolve three discrete episodes in data from a single sample. This is most likely when the first episode involves a maximum palaeotemperature sufficient to totally anneal all tracks (typically >110°C), followed by a subsequent peak around 90- 100°C which leads to shortening of tracks formed after the initial cooling to a mean length of ~10 μm. Finally, cooling to a low temperature is followed by reheating to ~70°C, sufficient to reduce track lengths formed after the second episode to ~12-13 μm.

Table 2 summarises estimates of peak palaeotemperatures reached by each sample and the time at which cooling from these palaeotemperatures began.

West Orkney Basin

Of six Permian-Lower Jurassic samples from offshore shallow boreholes in the WOB, most require two discrete episodes of heating and cooling (Table 2); an early episode involving cooling from palaeotemperatures typically >90°C beginning at some time during the mid-Jurassic to late Cretaceous (180 to 85 Ma based on combined results from all samples; Fig. 3). These palaeotemperatures imply significant depths of burial for any reasonable palaeogeothermal gradient. This was followed by reheating and a second cooling episode (from palaeotemperatures typically between 50- 70°C; Table 2) that commenced during the mid-late Cenozoic (between 30 and 15 Ma; Fig. 3). These results are interpreted in terms of burial of the preserved WOB succession by late Triassic-Jurassic sediments that were removed by exhumation that occurred in two stages (mid-Jurassic to late Cretaceous, and mid-late Cenozoic)

Exploration well 202/19-1

WOB well 202/19-1 was drilled in the hangingwall of the Solan Bank High Fault (Evans, 1997) and encountered ~3 km of Upper Permian-Lower Triassic sediments beneath a thin veneer of Quaternary deposits (Stoker et al, 1993). AFTA results indicate that all nine samples reached temperatures of ~100°C or above prior to cooling that began during the late Jurassic to late Cretaceous (Table 2), similar to results from WOB boreholes. The consistent timing of cooling based on overlap for all samples is 110 to 90 Ma (Fig. 3). A later episode of cooling beginning during the late Cretaceous-Cenozoic is also required for most samples, with the consistent overlap suggesting an onset beginning during the mid-late Cenozoic (55 to 10 Ma).

The variation of palaeotemperature with depth for the two separate episodes (Fig. 4b) suggests that both can be satisfied by linear palaeotemperature profiles, with gradients close to the present-day gradient of ~25.3°C km^{-1}. This indicates that these palaeotemperatures record heating caused by deeper burial and subsequent cooling caused by exhumation (cf. Green et al., 2002). Assuming a palaeosurface temperature of 5°C and palaeogeothermal gradients equivalent to the present-day gradient, early Cretaceous palaeotemperatures are consistent with deeper burial by 3.3-3.9 km of additional Triassic-Lower Cretaceous section, whilst the mid-late Cenozoic palaeotemperatures are consistent with an additional 1.2-1.7 km of section (Fig. 4c). Higher surface temperatures would require correspondingly lower amounts of additional section, while higher palaeogeothermal gradients (within the ranges allowed by the constraints on each episode) would require lower amounts of additional section.

Evans (1997) estimated the amount of deeper burial of the Permian-Triassic section at 202/19-1 by comparing Triassic shale sonic velocities against published velocity-depth relationships for normally compacted shales. By comparison with the burial curves of Marie (1975) and Magara (1976), Evans (1997) estimated gross exhumation of the Permian-Triassic section at 1.85 km. These velocity-depth relationships overestimate the increase of velocity with depth in comparison to more recent trends for Triassic shales from the British Isles (e.g. Japsen 2000). The value reported by Evans (1997) may thus underestimate the amount of gross exhumation by several hundred metres. The amount of exhumation indicated by sonic data is lower than that indicated by early Cretaceous AFTA palaeotemperatures assuming a geothermal gradient of 25.3°C km^{-1} (i.e. 3.3-3.9 km) but is reasonably close to the maximum likelihood value of additional section (2.31 km) (Fig. 4c). The slightly lower values of additional section indicated by the sonic velocity data could also indicate elevated basal heat flow during the early Cretaceous.

Based on AFTA and sonic data from 202/19-1 and AFTA data from shallow boreholes we suggest that up to 2-3 km of Upper Triassic-Lower Cretaceous sediments were deposited in parts of the WOB prior to early Cretaceous (110-90 Ma) exhumation. Although some samples are from footwall blocks, many others (including those from 202/19-1) are from hangingwalls which implies a regional cause for exhumation as opposed to localized exhumation of footwalls during Cretaceous normal faulting and extension.

Hebridean region

We analysed 22 samples from the North Minch Basin (NMB), Outer Hebrides and outcrops along the northwest coast of Scotland. Most require two palaeothermal episodes, and thermal history solutions for Permian and younger samples are generally similar to those resolved for basement samples (Table 2). When combined, results from this region reveal up to four separate cooling episodes during the Mesozoic-Cenozoic (Fig. 3).

Several of the Archean and Proterozoic samples, notably those in the footwalls of the NMB from Lewis and Harris and the northwest coast of Scotland, require Permian-Triassic cooling from temperatures generally >100°C (Table 2). An onset of cooling beginning between 225 and 190 Ma satisfies all samples that show evidence for this episode (Fig. 3).

Most samples from both basement and cover rocks in the Hebridean region show evidence for cooling from palaeotemperatures of up to ~105°C during the Jurassic to mid-Cretaceous (Table 2). Precise constraints on the timing of this episode are often broad in individual samples suggesting that Jurassic-mid Cretaceous cooling could result from several unresolved events, but Permian-Lower Cretaceous sedimentary samples from shallow boreholes in the Hebrides Shelf (GC523-47 to 52) define consistent evidence for cooling from ~90-95°C beginning during the early Cretaceous (140 to 130 Ma) (Fig. 3).

Likewise, most samples from the Hebridean region reveal evidence for elevated palaeotemperatures during the late Cretaceous-Cenozoic. Timing constraints are quite broad for some samples, which is again suggestive of several distinct phases of cooling that are closely spaced in temperature and time. It is possible to identify discrete late Cretaceous-mid Cenozoic and late Cenozoic cooling episodes in data from Permian-Triassic sample GC523-11 from NMB borehole 71/11. AFTA suggests that this sample cooled from 95-100°C between 75 and 30 Ma, with further cooling from 55-80°C between 15 Ma and the present-day. In Table 2 we have assigned late Cretaceous-Cenozoic cooling observed in individual episodes to discrete late Cretaceous-mid Cenozoic (75 to 40 Ma) and late Cenozoic (15 to 0 Ma) episodes, with the former more prevalent in basement samples on the flanks of the NMB (e.g. GC503-184) and the latter clearly resolved in samples from the Hebrides Shelf (e.g. GC523-49, 56). However, we acknowledge that other interpretations of these results are possible given the broad timing constraints for some samples.

Exploration well 134/5-1

We analysed eight AFTA samples from exploration well 134/5-1, located in the SOHB ~50 km southwest of Skye (Fig. 1). The well intersected ~2340 m of Upper Triassic-Lower Jurassic section intruded by numerous Palaeocene minor sills and dykes (i.e. <2 m thick). We also analysed 29 vitrinite reflectance (VR) samples (predominantly from the Jurassic section), using the kinetic model of Burnham and Sweeney (1989) to convert observed $R_o$max values to palaeotemperatures (using an assumed heating rate of 1°C Ma^{-1}).

BHT data indicate a present-day geothermal gradient of 47.5°C km^{-1}, but the DTH calculated on this basis for sample GC369-6 predicts total annealing, whereas this sample contains tracks and gives a finite (though very young) fission track age (Fig. 5a). In samples GC369-3 and 4 a similar comment applies to apatites containing <0.2 wt% Cl. In addition, GC369-4 and 5 show less length reduction than expected from the DTH. These aspects of the AFTA data suggest that present-day temperatures based on a gradient of 47.5°C km^{-1} are too high, and are more consistent with a gradient of ≤43°C km^{-1}. We have used this upper limit as the basis for construction of the DTH used to extract thermal histories from AFTA, and on this basis six samples show clear evidence of having been hotter in the past (Table 2).

Combining timing constraints derived from AFTA samples with maximum palaeotemperatures derived from VR data (Fig. 5b), indicates that two distinct Cenozoic cooling episodes have affected the preserved section (Table 2). VR-derived palaeotemperatures show fluctuations over narrow depth intervals around intrusions superimposed on a “background” linear profile (Fig. 5b). The rapid fluctuations clearly reflect contact heating around the igneous intrusions. AFTA data in GC369-2 is also interpreted to reflect contact heating, and a similar conclusion applies to the palaeotemperature constraint from GC369-1, as it plots above the main background trend defined by VR and other AFTA samples (Fig. 5b). AFTA data from the Triassic section (>1.75 km depth) define mid-Cenozoic cooling that began between 45 and 20 Ma (Table 2). Lower limits to the maximum palaeotemperature in this episode are consistent with the linear background trend defined by the VR data through this section and shallower units (Fig. 5b).

Similarly, the range of palaeotemperatures indicated by AFTA data in Jurassic sample GC523-58 is also consistent with this trend and palaeotemperatures indicated by VR data at similar depths. Therefore we interpret the "background" linear increase of palaeotemperature with depth indicated by the shallower and deeper VR data as defining a mid-Cenozoic palaeothermal peak (Fig. 3) Palaeotemperatures characterising this episode are consistent with a range of palaeogeothermal gradients from ~30-50 °C km^{-1} (Fig. 5c). If the mid-Cenozoic palaeogeothermal gradient was similar to the revised present-day gradient (43°C km^{-1}), these data imply deeper burial by between 0.64 to 0.91 km of additional post-Lower Jurassic section, removed during mid-Cenozoic (45-20 Ma) exhumation (Fig. 5c). These results confirm km-scale deeper burial of preserved Jurassic and Triassic strata, but also suggest that early Palaeocene cooling in some parts of this region, often attributed solely to exhumation, is dominantly a consequence of igneous activity.

Skye, Mull and Morvern

We analysed 31 onshore and two offshore samples collected on and around Skye, Mull and the Morvern peninsula, and one additional sample collected from central Scotland. Samples encompass a broad range of ages, from Mesoproterozoic to Upper Cretaceous (Fig. 3). Thermal history interpretation indicates that most samples around Skye, irrespective of their stratigraphic age (e.g. Moine sample GC523-6, near Glenancross and Jurassic sample GC523-10, from BH71/10) were totally annealed during early Palaeogene heating, reaching temperatures >110°C before cooling which began between 65 and 60 Ma (Fig. 3). Samples that were totally annealed during the early Palaeogene enable resolution of a late Cenozoic cooling episode, also observed in samples from Applecross that were not totally annealed in the Palaeocene event. Combining timing constraints for all samples suggests that cooling began between 20 and 10 Ma (Fig. 3). Results from around Mull are generally consistent with those from Skye, although the onset of Cenozoic cooling in Devonian sample GC523-77 from Iona and Moine sample GC523-78 from near Bunessan is slightly later (60 to 20 Ma) (Fig. 3). This could represent the failure to resolve two distinct Cenozoic cooling episodes.

AFTA results from Morvern are reported in more detail in a subsequent section of this paper, but generally define distinct cooling episodes beginning during the early-mid Triassic (245 to 225 Ma), early-mid Cenozoic (65 to 30 Ma) and late Cenozoic (20 to 10 Ma) (Table 2).

Integrating AFTA results with regional geological evidence

Triassic-early Jurassic cooling episodes (245-225 and 225-190 Ma)

Pre-Mesozoic samples across northwest Scotland provide evidence for two phases of cooling beginning during the Triassic-Jurassic. Lewisian basement samples from the Outer Hebrides (GC523-95, 97, 98) and Hebrides Shelf (GC523-55) reveal Triassic-early Jurassic cooling from >105°C that began between 225 and 190 Ma (Figs. 3, 6, 7a). There is no strong stratigraphic evidence for major Triassic-early Jurassic erosion in the Hebridean basins (Fyfe et al., 1993). Morton (1987) suggested that the first phase of crustal stretching responsible for the Hebridean basin system began ~210 Ma. Because these samples are located in the footwalls of major Triassic-Jurassic normal faults (e.g. the Minch Fault; Roberts & Holdsworth, 1999) we interpret this cooling as due to localized exhumation driven by footwall uplift. Similar footwall uplift has been identified in the North Sea from seismic data (Roberts & Yielding, 1991), although any palaeothermal effects there have been overprinted by Jurassic burial, reflecting the greater degree of extension and post-rift subsidence.

Mesoproterozoic (Moine), Silurian (Strontian Granite) and Devonian sedimentary AFTA samples from around Skye, Mull and Morvern reveal evidence for early Triassic cooling that began between 245 and 225 Ma (Figs. 3, 6, 7a). Sample RD17-41 also shows that cooling at this time also occurred in central Scotland, emphasising the regional extent of this episode (Fig. 7a). Whilst the timing of cooling is similar to that observed in the footwall of the Minch Fault (e.g. samples GC523-95, 97, 98), the consistency of data and interpretations over much of the study area (Tables 1 and 2, Fig. 3) suggests a more regional event. One possible explanation for this early Triassic cooling is that it represents the final stage of post-Caledonian unroofing that brought Precambrian and Lower Palaeozoic basement rocks to the surface prior to their reburial beneath Mesozoic sediments.

Early-mid Cretaceous cooling episodes (140-130 and 110-90 Ma)

A key finding of this study is that Permian-Lower Cretaceous sediments now exposed at or near surface levels around northwest Scotland have been heated to temperatures higher than 90-100°C which we interpret as reflecting regional Triassic-Jurassic burial. Particularly in northern and central parts of the study area (e.g. the WOB), these maximum post-depositional temperatures were attained during the early to mid-Cretaceous (Figs. 3, 7b, c).

Our results indicate two separate phases of early Cretaceous cooling, with the more recent event apparently restricted to the WOB (including well 202/19-1) while the earlier event affected a wider region, across the Hebrides and eastwards into central Scotland (Fig. 7b). Our preferred interpretation is that these are distinct episodes based on consistencies in the data that characterise the different events (Tables 1 and 2). Early Cretaceous cooling is less well defined around Skye, Mull and Morvern (Fig. 7b), which we attribute to overprinting by early Palaeogene heating related to igneous activity. Results from well 202/19-1 suggests that heating to the early to mid-Cretaceous palaeotemperatures was dominantly due to deeper burial, with subsequent cooling to exhumation, and this conclusion can be extended to cooling at this time recorded in WOB shallow borehole samples (Table 2; Fig. 3).

Cretaceous rocks are largely absent around northwest Scotland, but where preserved their stratigraphic relations often provide evidence for early-mid Cretaceous exhumation and deformation. Cenomanian sandstones at Morvern rest unconformably on Lower Jurassic and older rocks, indicating intervening uplift and erosion (Fyfe et al, 1993). In north Skye, NE-trending anticlines within Jurassic strata are not observed in the thin Upper Cretaceous sequences that underlie Paleocene lavas (England, 1994). The axes of these folds trend parallel to the major basin-bounding faults (e.g. the Camasunary-Skerryvore Fault), and indicate early Cretaceous deformation in the Hebridean region (Bell & Williamson, 2002). Further south, AFTA data from wells in the Irish Sea basin system and from samples onshore Ireland record widespread early Cretaceous (~120-115 Ma) exhumation (Holford et al., 2009a). AFTA and compaction data from the Lower Jurassic succession of the Mochras borehole indicate ~2.5 km of early Cretaceous exhumation at that location (Holford et al., 2005). These observations confirm the regional nature of early Cretaceous cooling and exhumation, although slight differences in the timing of cooling between individual areas results in some uncertainty with regards to identification of discrete episodes and their correlations with events in the stratigraphic record.

Early Cenozoic (65-60 Ma)

Early Cenozoic exhumation of northern Scotland is thought to be a source of Palaeocene sediments in the Faroe-Shetland Basin (White & Lovell, 1997; Stoker et al., 2010), and a number of previous studies have suggested regional Palaeocene uplift and exhumation across northern Scotland based either on thermochronology (Persano et al., 2007) or geophysical studies (Jones et al., 2002). However, our AFTA data shows that early Cenozoic cooling is restricted dominantly to the vicinity of Palaeogene igneous centres (e.g. Skye, Mull) (Fig. 7c). Away from these intrusions, early Cenozoic palaeotemperatures decrease rapidly, whilst some regions such as the WOB show no obvious requirement for early Cenozoic cooling (Fig. 7b), and earlier or later cooling episodes dominate the thermal histories.

The clearest evidence for elevated early Cenozoic palaeotemperatures is provided by Jurassic AFTA samples from Skye, where all but one sample show evidence for palaeotemperatures >110°C prior to cooling beginning between 65 and 60 Ma (Table 2). This is consistent with previous results from Skye that also reveal early Cenozoic palaeotemperatures >110°C (Lewis et al., 1992). In contrast, VR data from onshore Middle Jurassic sediments in the Inner Hebrides signify localized elevated palaeotemperatures around contemporaneous igneous intrusions, while away from intrusive bodies VR values are much lower (Hudson and Andrews, 1987). The compaction and cementation state of these sandstones suggest maximum burial depths of only ~1 km (Hudson and Andrews, 1987), indicating that the early Cenozoic palaeotemperatures of >110°C revealed by AFTA most likely do not reflect solely deeper burial, but are more likely due to hydrothermal and/or contact heating, similar to that observed in the 134/5-1 well (Fig. 5c) Thus, whilst early Cenozoic cooling recorded by AFTA data in some samples may in part record regional exhumation, over much of this region it is difficult to isolate this signal from thermal effects related to igneous activity. But in other areas (e.g. WOB) early Cenozoic exhumation is clearly of lower magnitude than that during the early Cretaceous and mid-late Cenozoic.

Mid-Cenozoic (45-20 Ma)

Data from 134/5-1 and 202/19-1 reveal evidence for mid-Cenozoic cooling. Samples from 134/5-1 provide the most detailed definition of this episode, showing cooling beginning between 45 and 20 Ma and indicating exhumation of Lower Jurassic and older rocks involving removal of ~0.6-0.9 of additional section (Fig. 5). Results from 202/19-1 are consistent with a similar timing, while requiring a larger amount of removed section. This cooling and exhumation is contemporaneous with a regional Upper Eocene (~34±3 Ma) unconformity reported from the Atlantic margin (Praeg et al., 2005) and coeval with progradation of early Oligocene clastic wedges into the eastern North Sea, which is taken to record the onset of Scandinavian uplift (Japsen et al., 2007). Jolivet (2007) provides evidence for similarly timed (40-25 Ma) cooling onshore Scotland recorded by apatite fission track data from Loch Ness and Strontian. Jolivet (2007) interpreted this data in terms of ~1.6 to 2 km of post mid-Cenozoic denudation.

There are at least three outliers of late Oligocene terrestrial sediments within our study area (Fig. 1). Sediments reach a maximum thickness of ~1 km in the Canna Basin, and in all areas are variably tilted and folded, and overlain with marked unconformity by Quaternary deposits (Fyfe et al., 1993). Lithologies (freshwater mudstones, sandstones and lignites) are similar to other Oligocene terrestrial deposits in western Britain (e.g. Lough Neagh, Cardigan Bay basins). Compaction and palaeothermal data show that these sediments have been exhumed by up to 1.5 km (Holford et al., 2005, 2009b). No such data exist for the Oligocene outliers offshore Scotland, but their preservation and deformation point to complex local variations in mid-Cenozoic vertical motions.

Late Cenozoic (15-10 Ma)

Most AFTA samples reveal major late Cenozoic cooling from palaeotemperatures of ~60-65°C to their present-day temperatures (Fig. 7d; Table 1). Data from most regions are consistent with a regionally synchronous onset between 15 and 10 Ma (Fig. 3, 6). AFTA samples from the WOB suggest an earlier (30-15 Ma) onset, although this could represent the combined effects of mid and late Cenozoic cooling. In contrast to earlier uplift episodes where there is often uncertainty as to the amount of subsequent reburial, we can quantify the amount of reburial following late Cenozoic uplift because Quaternary sedimentary thicknesses are well constrained (generally <100 m) (e.g. Fyfe et al., 1993; Stoker et al., 1993). We use late Cenozoic palaeotemperatures to estimate amounts of exhumation since the late Cenozoic. Gross exhumation estimates (i.e. uncorrected for reburial) have been calculated using minimum, maximum and mid-point palaeotemperature estimates, assuming a late Cenozoic palaeosurface temperature of 10°C and late Cenozoic palaeogeothermal gradients that decrease linearly from 43°C km^{-1} at 134/5-1 to 25.3°C km^{-1} at 202/19-1 (i.e. similar to the present-day gradients) (Fig. 8). Estimates based on mid-point palaeotemperatures show a consistent northwards increase, with lowest values (>0.92 km) in the vicinity of Skye, and highest values (<1.94 km) in the WOB (Fig. 8). Estimates from the WOB are similar to late Cenozoic exhumation estimates across the southern British Isles from AFTA and sonic velocity data (Holford et al., 2005, 2009a). Around major igneous centres (e.g. Mull), a significant fraction of the section eroded during the late Cenozoic may have comprised lavas that accumulated during the Palaeocene (cf. Walker, 1971).

Integration of AFTA data with stratigraphic constraints on the Morvern peninsula

Fourteen AFTA samples have been analysed from Morvern (Fig. 9), where sedimentary rocks of Mesoproterozoic (Moine metasediments; samples GC523-2, RD17-43), Upper

Carboniferous (GC523-72 & 74), Triassic (GC523-1 & 3), Lower Jurassic and Upper Cretaceous (Cenomanian-?Santonian; GC523-4 & 5) ages crop out within an area of ~20 km^2. In addition there is a ~460 m thick succession of the Palaeocene Mull Lava Group, whilst the eastern part of the peninsula comprises Silurian Strontian granite (RD17-42, 44 to 48). This area provides a unique opportunity to integrate stratigraphic constraints with thermal history information from AFTA to evaluate burial and uplift histories of basement and cover rocks. In basement terrains without younger sedimentary cover, the only available thermal history constraints for modelling of fission track data are the measured present-day temperature and an assumed depositional/metamorphic/crystallisation temperature. However, Moine rocks on Morvern are variably overlain by Triassic, Lower Jurassic and Upper Cretaceous sediments, showing that the basement rocks now exposed across this region had been exhumed to near-surface levels/temperatures at these times.

The Upper Triassic sandstones from which samples GC523-1 and 3 were collected unconformably overlie Moine Supergroup metasediments, while the Silurian Strontian Granite outcrops nearby (Fig. 9a). These pre-Caledonian rocks must therefore have been exhumed to surface levels by the late Triassic, at which time a regional planation surface had been created, now represented by the sub-Triassic unconformity. Samples of Moine and Strontian Granite from Morvern consistently record cooling from >100°C that began between 245 and 225 Ma (Table 2). In other words, samples now just below the level of the unconformity were at paleotemperatures >100°C a few Myr prior to the time at which they reached that position and the overlying Upper Triassic sedimentary units were deposited. Therefore we interpret the early Triassic cooling episode as representing the period of exhumation that led to formation of the unconformity underlying the Upper Triassic sediments (Fig. 9c).

The Upper Triassic sandstones are conformably overlain by Lower Jurassic sandstones and shales, in turn unconformably overlain by the ~20 m thick Cenomanian (possibly Turonian) marginal marine Loch Aline White Sandstone Formation, indicating the presence of a Cenomanian coastline (Lowden et al., 1992). The absence of Middle Jurassic to Early Cretaceous section indicates a period of erosion or non-deposition during this interval. AFTA data from Morvern provide no direct evidence for cooling associated with this unconformity (Fig. 9c). But as Jurassic heating and burial and early Cretaceous cooling, exhumation and deformation is observed in northern parts of our study area we suggest it is also likely to have occurred in Morvern, but palaeotemperatures associated with this episode were subsequently overprinted by higher early Cenozoic paleotemperatures (below).

Most samples of Moine and Strontian Granite, as well as the two samples of Upper Triassic sandstone, record reheating to ~80-90°C or above in the early Cenozoic (Table 2). This event is also recorded in samples GC523-4 and 5 from the Loch Aline Sandstone (Table 2), which show that following deposition at ~95 Ma, it was heated to 90-105°C in the Early Cenozoic. Over 100 m of Upper Carboniferous (Westphalian) sandstones and mudstones occur in a faulted inlier on the southern coast of Morvern. While the relationship between this and younger units is not clear, thermal histories of AFTA samples GC523-72 and 74 are similar to the Cenomanian samples, defining early Cenozoic palaeotemperatures of ~100°C (Fig. 9c).

As noted earlier, early Cenozoic paleotemperatures across the study region are interpreted as dominantly reflecting processes related to igneous activity, chiefly contact and hydrothermal effects as well as locally elevated heat flow and possibly deeper burial, and the effects of these competing processes cannot be resolved. But if the early Cenozoic paleotemperatures in these samples involved any degree of deeper burial, it is clear that the entire section must have been reburied following deposition of the Cenomanian sandstone, to achieve these early Cenozoic palaeotemperatures. Burial beneath a late Cretaceous Chalk cover seems plausible. While Upper Cretaceous strata are poorly represented in this area, sediments of this age are identified in Skye, Raasay and Eigg, and Chalk Group fragments of possible Campanian age occur in volcanic vents in Arran (Fyfe et al., 1993). If such burial occurred, early Palaeocene exhumation must have occurred to produce the predominantly subaerial landsurface onto which lavas and pyroclastic material were erupted (Emeleus & Bell, 2005). Alternatively, early Cenozoic palaeotemperatures could be related to hydrothermal and other effects associated with volcanic activity during or subsequent to extrusion of lavas, although in this case, reheating from near-surface temperatures is still required (Fig. 9c).

Late Cenozoic (20-10 Ma) paleotemperatures around 60-70°C are also recorded in almost all samples from Morvern, as well as other areas in this study (although results in some samples from Morvern may represent the unresolved effects of both early and late Cenozoic episodes; Table 2). The presence of the volcanic sequence and the underlying sub-aerial surface shows that the section must have been re-buried. The Mull Lava Group has a thickness of ~460 m on Morvern, and zeolite minerals (e.g. mesolite, laumonite) within the lavas indicate this area may have been buried by >1 km of additional lavas (Bell & Williamson, 2002). The depth-related zeolite zones are superimposed on hydrothermal mineral zones related to the Mull Central Complex (Bell & Williamson, 2002), and a zone of Carbonate minerals on western Morvern is interpreted to have been deposited by circulating heated waters from the Ardnamurchan Central Complex (Walker, 1971).

Integration of AFTA data from various stratigraphic levels with geological evidence thus reveal a complex history of post-Caledonian vertical motions across Morvern (Figure 9c). Moine basement rocks have been repeatedly buried then exhumed to surface levels, and at least three major cycles of heating and cooling have been identified. This is in stark contrast to the monotonic post-Caledonian cooling histories proposed for this region by thermochronological studies that have focused on basement rocks rather than younger sedimentary cover (e.g. Persano et al., 2007). We suggest that such episodic histories are unlikely to be restricted to this one location, and that such histories are likely to be the rule, rather than the exception.

Discussion

New AFTA data from northwest Scotland reveal a complex history of vertical motions characterized by multiple cycles of Mesozoic-Cenozoic burial and exhumation (Fig. 10). Our data reveal regional cooling and uplift episodes that began during the early-mid Triassic (245-225 Ma), early Cretaceous (140-120 Ma), early Cenozoic (65-60 Ma), mid Cenozoic (45-20 Ma) and late Cenozoic (15-10 Ma) (Fig. 3, 6). AFTA data in Permian-Mesozoic units from offshore wells allow evaluation of palaeogeothermal gradients and indicate that deeper burial is the primary cause of heating, and that exhumation is the main cause of cooling in these episodes, except for early Cenozoic heating which appears in large part to be related to igneous activity. The Cenozoic history of uplift and erosion is consistent with the offshore sedimentary record to the north and west of our study area, with multiple tectonically-influenced sedimentation pulses of Palaeocene, Eocene, Oligocene, Miocene and Plio-Pleistocene observed in the Rockall and Faroe-Shetland basins (Stoker et al, 2010). Our results, which indicate a major role for Cenozoic tectonics in the development of the Scottish landscape, are worth comparing with recent geomorphological studies of Ireland (Dewey, 2000), which indicate that many topographic features may owe their origin due to faults active during Palaeogene extension and Neogene compression.

Jurassic sedimentary cover over the Highlands?

A key aspect of our results is that many Permian-Triassic samples appear to have reached temperatures of 90-100°C or above in the early Cretaceous. Samples of basement and Palaeozoic sediments give comparable results, implying similar geological histories for basement terrains and sedimentary basins over the past ~200 Myr. The sedimentary basins of the Hebrides contain thick successions of marine Jurassic rocks (e.g. ~2.5 km in the NMB; Fyfe et al., 1993), and our results imply that comparable successions were deposited where Jurassic rocks are now missing, including across the northern Highlands. Sequence-stratigraphic analyses of Middle-Upper Jurassic marine sediments in the Inner Moray Firth and Hebridean basins reveal stratigraphic affinities that imply a marine connection (Underhill and Partington, 1993). Underhill (1991) postulated that such a connection may have existed along the trace of the Great Glen Fault. Roberts & Holdsworth (1999) argued that the Highlands were traversed by a component of Mesozoic extension along NNE-SSW trending faults, and that many structures that are traditionally held to be Caledonian may in fact be of Mesozoic age. Quartz-filled fractures within Cambrian rocks west of the Moine Thrust Zone provide independent evidence for Mesozoic extension (Laubach & Diaz-Tushman, 2009). These fractures strike N-NE and are associated with post-Caledonian faults, leading Laubach & Diaz-Tushman (2009) to attribute their formation to Mesozoic extension. Fluid inclusion homogenization temperatures show these fractures formed at ~80°C, in good agreement with early Mesozoic palaeotemperatures predicted by thermal modelling of AFTA samples that from the northwest coast (Fig. 7b). AFTA indicate that a maximum of 2-3 km of Jurassic sediments have been removed from northern parts of the Hebridean basin system (e.g. the

West Orkney Basin) during post-Jurassic exhumation. Lower exhumation is likely in southern areas where thicker Mesozoic sequences are preserved (e.g. in the vicinity of Skye, where a thick Jurassic succession is preserved, diagenetic evidence suggests deeper burial of these rocks by ~1 km (Hudson & Andrews, 1987)

Implications for low-temperature thermal histories of basement regions

The repeated cycles of heating and cooling revealed by our data and implied by the geological record are in marked contrast to the results of a recent study that presented apatite fission-track and (U-Th)/He (AHe) data from two locations in northwest Scotland; Clisham (Achaean gneisses) and Sgorr Dhonuill (Silurian granites) (Persano et al., 2007). Persano et al. (2007) interpreted their data as recording continuous, monotonic cooling over the past 400 My (i.e. consistent with continuous post-Caledonian emergence), with an early Cenozoic acceleration in cooling. Their approach was based on forward modelling of fission-track and AHe data to indentify thermal histories that were consistent with the observed fission track and AHe ages.

Persano et al (2007) extracted thermal history constraints from their AHe data using the systematics of He diffusion in apatite defined for Durango apatite by Farley (2000). Although these systematics have been widely adopted, recent studies have shown that He diffusion in apatite is more complicated than originally supposed. Green at al. (2006) reported systematic inconsistencies between measured AHe ages and values predicted on the basis of thermal histories derived from AFTA using the Farley (2000) systematics, with discrepancies increasing with U content of the apatite and the fission track age. Further empirical data showing similar effects (Flowers et al., 2007), combined with new experimental investigations of AHe diffusion kinetics (Shuster et al., 2006) have shown that apatite becomes more retentive of He as radiation damage accumulates within the crystal lattice. Consequently, apatites with high effective U (eU) concentrations and older fission track ages retain He at much higher temperatures than young apatites with low eU concentrations such as Durango apatite (Shuster et al., 2006). Because Persano et al. (2007) did not consider the effects of radiation damage, the thermal history interpretations they derive from the AHe data cannot be considered reliable. For all samples where Persano et al. (2007) report both AHe and fission track ages, the latter are considerably older than 100 Ma (the youngest being a value of 186±6 Ma sample in SD9), and so the interpretation of the AHe data in these samples by Persano et al. (2007) using the Farley (2000) systematics in terms of an early Cenozoic acceleration in cooling is unlikely to be valid (Green et al., 2006).

Even if this interpretation was accurate, it is far from straightforward to attribute early Cenozoic cooling solely to regional exhumation, given the results here which suggest a link to contemporaneous igneous activity (Fig. 2, 5b). Whilst it remains possible that regional Palaeocene exhumation may contribute to early Cenozoic cooling, further work is needed to isolate this signal from cooling resulting from the cessation of hydrothermal heating, contact effects and more localised exhumation caused by intrusion of central complexes (Brown et al., 2009).

Low-temperature thermochronological studies of basement rocks from onshore passive margins and continental interiors commonly assume monotonic cooling (e.g. Dempster & Persano, 2006). However, our results, best demonstrated by samples from the Morvern peninsula (Fig. 9), indicate that episodic histories dominated by repeated cycles of heating and cooling (i.e. burial and exhumation) are more realistic. The common assumption of monotonic cooling histories for low temperature thermochronological studies is only possible occurs because such studies traditionally focus on basement rocks and ignore the significance of any sedimentary outliers that may be present (Green and Duddy, 2007). We suggest that this naive approach can lead to erroneous conclusions, and is no longer tenable.

Origin of uplift episodes

A synthesis of AFTA data from multiple wells and outcrops in the Irish Sea basins by Holford et al. (2009a) identified regional (up to ~10^6 km^2) exhumation-driven cooling episodes beginning during the early Cretaceous and the early, mid and late-Cenozoic that can be correlated with the episodes observed in northwest Scotland. These results suggest greater complexity than previous studies that have suggested that exhumation across the western British Isles is dominantly Palaeogene in age, driven by plume-related igneous underplating (Brodie & White, 1994; White & Lovell, 1997; Jones et al., 2002; Persano et al., 2007). Whilst underplating may well have contributed to the localized early Palaeogene exhumation around Hebridean igneous centres, underplating and dynamic uplift cannot explain the Triassic and early Cretaceous exhumation of northwest Scotland, and we consider it unlikely that the mid and late Cenozoic exhumation episodes constrained by our AFTA data were primarily plume-driven.

Holford et al. (2009a) noted close temporal relationships between the onset of Cretaceous-Cenozoic exhumation episodes across the western British Isles and plate boundary reorganizations associated with the North Atlantic oceanic ridge system, and increased periods of convergence and coupling between the Eurasian and African plates associated with Alpine collision. These correlations suggest that increased levels of intraplate stress propagated from plate boundary interactions may explain the exhumation episodes constrained by AFTA data. Present-day stress data from northwest Europe indicate a northwest-southeast orientation of maximum horizontal stress in the upper crust consistent with control by plate boundary forces (Goelke & Coblentz, 1996). Cenozoic compressional stress magnitudes in particular are likely to have been high (perhaps ~100 MPa) due to ridge push forces enhanced by anomalously high temperature asthenosphere underlying the elevated northeast Atlantic spreading axis, which is above sea level at Iceland (Bott, 1993; Doré et al., 2008). High magnitudes of intraplate stress can explain the large number of Cretaceous-Cenozoic compressional structures in post-Palaeozoic basins of the British Isles and Atlantic Margin that contain weak sedimentary infills (Hillis et al., 2008). It may also explain uplift of 'uninverted' basement regions due to the distributed effects of relatively low strain rates ($<10^{-16}$ s^{-1}) operating over timescales of >1-10 Myr. The resultant cumulative crustal shortening, although relatively minor (<5-10%) may nonetheless be sufficient to generate long-wavelength uplift and exhumation. Low degrees of crustal shortening have been invoked to explain late Cenozoic uplift and deformation of other intraplate regions e.g. the West Siberian Basin (Allen & Davies, 2007) and the margins of the Australian continent (Sandiford et al., 2004).

Conclusions

We have constrained post-Caledonian vertical motions around northwest Scotland using 78 AFTA samples from onshore outcrops, and offshore shallow boreholes and deep exploration wells. Samples came from both Proterozoic-Lower Palaeozoic basement and Mesozoic cover sequences. Our results indicate multiple Mesozoic-Cenozoic cooling and exhumation episodes, several of which correlate with similar events recorded by AFTA data throughout western Britain. Thermal histories of basement and cover samples are generally consistent, and many Permian-Triassic samples cooled from temperatures of 90-100°C or above during the Cretaceous. These results require deposition of considerable additional thicknesses of

Triassic-Jurassic rocks in the Hebridean basins, and suggest deposition of Mesozoic sediments across the Highlands. This additional cover was removed during regional early Cretaceous and mid-late Cenozoic exhumation. AFTA data record early Cenozoic heating and cooling, but it is difficult to isolate the contribution by regional uplift from thermal effects associated with igneous activity. Combined with preserved stratigraphy which records intermittent Upper Palaeozoic-Mesozoic sedimentation across northwest Scotland, our data are incompatible with a significant Caledonian component in the present-day topography. Instead, tectonic processes have repeatedly uplifted northwest Scotland over the past ~140 Myr and erosion has stripped away a considerable thickness of cover. Our results emphasize the importance of integrating thermal history data from basement and overlying sedimentary units when reconstructing the uplift histories of onshore passive margins and intraplate regions, and also demonstrate the importance of integrating observations from onshore and offshore.

Acknowledgements

This work forms part of ARC Discovery Project DP0879612, and represents TRaX contribution #75. We thank Alan Roberts and an anonymous reviewer for their comments and Tim Needham for editorial guidance. The contribution of Stoker is made with the permission of the Executive Director, British Geological Survey (Natural Environment Research Council).

References

ALLEN, M.B. & DAVIES, C.E. 2007. Unstable Asia: active deformation of Siberia revealed by drainage shifts. *Basin Research,* **19,** 379-392.

BELL, B.R. & WILLIAMSON, I.T. 2002. Tertiary igneous activity. *In:* TREWIN, N.H. (ed) *The Geology of Scotland.* 4th edition. Geological Society, London, 371-408.

BOTT, M.H.P. 1993. Modelling the plate-driving mechanism. *Journal of the Geological Society, London,* **150,** 941-951.

BRODIE, J. & WHITE, N. 1994. Sedimentary basin inversion caused by igneous underplating. *Geology,* **22,** 147-150.

BROWN, D.J., HOLOHAN, E.P. & BELL, B.R. 2009. Sedimentary and volcano-tectonic processes in the British Paleocene Igneous Province: a review. *Geological Magazine,* **146,** 326-352.

BURNHAM, A.K. & SWEENEY, J.J. 1989. A chemical kinetic model of vitrinite reflectance and maturation. *Geochimica et Cosmochimica Acta,* **53,** 2649-2657.

CHADWICK, R.A. & PHAROAH, T.C. 1998. The seismic reflection Moho beneath the United Kingdom and adjacent areas. *Tectonophysics*, **299**, 255-279.

DEMPSTER, T.J. & PERSANO, C. 2006. Low-temperature thermochronology: Resolving geotherm shapes or denudation histories? *Geology,* **34,** 73-76.

DEWEY, J.F. 2000. Cenozoic tectonics of western Ireland. *Proceedings of the Geologists' Association,* **111,** 291-306.

DORÉ, A.G., CARTWRIGHT, J.A., STOKER, M.S., TURNER, J.P. & WHITE, N.J. 2002. Exhumation of the North Atlantic margin: introduction and background. *In*: DORÉ, A.G., CARTWRIGHT, J.A., STOKER, M.S., TURNER, J.P. & WHITE, N. (eds) *Exhumation of the North Atlantic Margin: Timing, Mechanisms and Implications for Petroleum Exploration.* Geological Society, London, Special Publications, **196,** 1-12.

DORÉ, A.G., LUNDIN, E.R., KUSZNIR, N.J. & PASCAL, C. 2008. Potential mechanisms for the genesis of Cenozoic domal structures on the NE Atlantic margin: pros, cons and some new ideas. *In:* JOHNSON, H., DORÉ, A. G., GATLIFF, R. W., HOLDSWORTH, R., LUNDIN, E. & RITCHIE, J. D. (eds) The Nature and Origin of Compression in Passive Margins. Geological Society, London, Special Publications, **306,** 1–26.

EMELEUS, C. H. & BELL, B. R. 2005. *The Palaeogene volcanic districts of Scotland.* 4th ed. British Geological Survey, Nottingham.

ENGLAND, R.W. 1994. The structure of the Skye lava field. *Scottish Journal of Geology,* **30,** 33-37.

EVANS, D.J. 1997. Estimates of the eroded overburden and the Permian-Quaternary subsidence history of the area west of Orkney. *Scottish Journal of Geology,* **33,** 169-182.

FARLEY, K.A. 2000. Helium diffusion from apatite: General behaviour as illustrated by Durango fluorapatite. *Journal of Geophysical Research,* **105B,** 2903-2914.

FLOWERS, R.M., SHUSTER, D.L., WERNICKE, B.P. & FARLEY, K.A. 2007. Radiation damage control on apatite (U-Th)/He dates from the Grand Canyon region, Colorado Plateau. *Geology*, **35,** 447-450.

FYFE, J. A., LONG, D. & EVANS, D. 1993. *United Kingdom offshore regional report: The Geology of the Malin-Hebrides Sea Area*. British Geological Surey, London, Her Majesty's Stationary Office.

GALBRAITH, R.F. & LASLETT, G.M. 1993. Statistical methods for mixed fission track ages. *Nuclear Tracks*, **21**, 459-470.

GALLAGHER, K. 1995. Evolving temperature histories from apatite fission-track data. *Earth and Planetary Science Letters*, **136,** 421-435.

GEIKIE, A. 1901. *The Scenery of Scotland.* London.

GEORGE, T.N. 1966. Geomorphic evolution in Hebridean Scotland. *Scottish Journal of Geology*, **2,** 1-34.

GÖLKE, M. & COBLENTZ, D. 1996. Origins of the European regional stress field. *Tectonophysics*, **266,** 11-24.

GREEN, P.F. 1986. On the thermo-tectonic evolution of Northern England: evidence from fission track analysis. *Geological Magazine*, **123**, 493-506.

GREEN, P.F. & DUDDY, I.R., 2007. Discussion on 'Apatite (U – Th)/He age constraints on the Mesozoic and Cenozoic evolution of the Bathurst Region, New South Wales: evidence for antiquity of the continental drainage divide along a passive margin'. *Australian Journal of Earth Sci*ences, **54**, 1009–1011.

GREEN, P.F., THOMSON, K. & HUDSON, J.D. 2001. Recognizing tectonic events in undeformed regions: contrasting results from the Midland Platform and East Midlands Shelf, Central England. *Journal of the Geological Society, London,* **158,** 59-73.

GREEN, P.F., DUDDY, I.R. & HEGARY, K.A. 2002. Quantifying exhumation in sedimentary basins of the UK from apatite fission track analysis and vitrinite reflectance data: precision, accuracy and latest results. *In*: DORÉ, A.G., CARTWRIGHT, J.A., STOKER, M.S., TURNER, J.P. & WHITE, N. (eds) *Exhumation of the North Atlantic Margin: Timing, Mechanisms and Implications for Petroleum Exploration.* Geological Society, London, Special Publications, **196,** 331-354.

GREEN, P.F., CROWHURST, P.V., DUDDY, I.R., JAPSEN, P. & HOLFORD, S.P. 2006. Conflicting (U-Th)/He and fission track ages in apatite: Enhanced He retention, not anomalous annealing behaviour. *Earth and Planetary Science Letters,* **250,** 407-427.

HALL, A.M. 1991. Pre-Quaternary landscape evolution in the Scottish Highlands. *Transactions of the Royal Society of Edinburgh: Earth Sciences,* **82,** 1-26.

HALLAM, A. 1983. Jurassic, Cretaceous and Tertiary sediments. *In:* CRAIG, G.Y. (ed) *Geology of Scotland.* 2nd edition. Scottish Academic Press, Edinburgh, 343-356.

HILLIER, S. & MARSHALL, J.E.A. 1992. Organic maturation, thermal history and hydrocarbon generation in the Orcadian Basin, Scotland. *Journal of the Geological Society, London,* **149,** 491-502.

HILLIS, R.R., HOLFORD, S.P., GREEN, P.F., DORÉ, A.G., GATLIFF, R.W., STOKER, M.S., THOMSON, K., TURNER, J.P., UNDERHILL, J.R. & WILLIAMS, G.A. 2008. Cenozoic exhumation of the southern British Isles. *Geology,* **36,** 371-374.

HOLFORD, S.P., GREEN, P.F. & TURNER, J.P. 2005. Palaeothermal and compaction studies in the Mochras borehole (NW Wales) reveal early Cretaceous and Neogene exhumation and argue against regional Palaeogene uplift in the southern Irish Sea. *Journal of the Geological Society, London,* **162,** 829-840.

HOLFORD, S.P., GREEN, P.F., DUDDY, I.R., TURNER, J.P., HILLIS, R.R. & STOKER, M.S. 2009a. Regional intraplate exhumation episodes related to plate boundary deformation. *Geological Society of America Bulletin,* **121,** 1611-1628, doi: 10.1130/B26481.1

HOLFORD, S.P., GREEN, P.F., HILLIS, R.R., TURNER, J.P. & STEVENSON, C.T.E. 2009b. Mesozoic-Cenozoic exhumation and volcanism in Northern Ireland constrained by AFTA and compaction data from the Larne No. 2 borehole. *Petroleum Geoscience,* **15,** 239-257.

HUDSON, J.D. & ANDREWS, J.E. 1987. The diagenesis of the Great Estuarine Group, Middle Jurassic, Inner Hebrides, Scotland. *In:* Marshall, J.D. (ed.) *Diagenesis of Sedimentary Sequences.* Geological Society, London, Special Publications, **36,** 259-276.

HURFORD, A.J. & GREEN, P.F. 1983. The zeta age calibration of fission-track dating. *Chemical Geology,* **1,** 285-317.

JAPSEN, P. 2000. Investigation of multi-phase erosion using reconstructed shale trends based on sonic data, Sole Pit axis, North Sea. *Global and Planetary Change,* **24,** 189-210.

JAPSEN, P., BIDSTRUP, T. & LIDMAR-BERGSTRÖM, K. 2002. Neogene uplift and erosion of southern Scandinavia induced by the rise of the South Swedish Dome. *In*: DORÉ, A.G., CARTWRIGHT, J.A., STOKER, M.S., TURNER, J.P. & WHITE, N. (eds) *Exhumation of the North Atlantic Margin: Timing, Mechanisms and Implications for Petroleum Exploration.* Geological Society, London, Special Publications, **196,** 183-207.

JAPSEN, P., GREEN, P.F., HENRIK NIELSEN, L., RASMUSSEN, E.S. & BIDSTRUP, T., 2007. Mesozoic-Cenozoic exhumation events in the eastern North Sea Basin: a multi-disciplinary study based on paleothermal, palaeoburial, stratigraphic and seismic data. *Basin Research,* **19,** 451-490.

JOLIVET, M. 2007. Histoire de la denudation dans le corridor du loch Ness (Écosse): mouvements verticaux différentiels le long de la Great Glen Fault. *Comptes Rendus Geoscience,* **339,** 121-131.

JONES, S.M., WHITE, N., CLARKE, B.J., ROWLEY, E. & GALLAGHER, K. 2002. Present and past influence of the Iceland Plume on sedimentation. *In*: DORÉ, A.G., CARTWRIGHT, J.A., STOKER, M.S., TURNER, J.P. & WHITE, N. (eds) *Exhumation of* *the North Atlantic Margin: Timing, Mechanisms and Implications for Petroleum Exploration.* Geological Society, London, Special Publications, **196,** 13-25.

LAUBACH, S.E. & DIAZ-TUSHMAN, K. 2009. Laurentian palaeostress trajectories and ephemeral fracture permeability, Cambrian Eriboll Formation sandstones west of the Moine Thrust Zone, NW Scotland. *Journal of the Geological Society, London,* **166,** 349-362.

LEWIS, C. L. E., CARTER, A. & HURFORD, A.J. 1992. Low temperature effects of the Skye Tertiary intrusions on Mesozoic sediments in the Sea of Hebrides Basin. *In:* PARNELL, J. (ed) *Basins on the Atlantic Seaboard: Petroleum Geology, Sedimentology and Basin Evolution.* Geological Society, London, Special Publications, **62,** 64-77.

LOWDEN, B., BRALEY, S., HURST, A. & LEWIS, J. 1992. Sedimentological studies of the Cretaceous Lochaline Sandstone, NW Scotland. *In:* PARNELL, J. (ed) *Basins on the Atlantic Seaboard: Petroleum Geology, Sedimentology and Basin Evolution.* Geological Society, London, Special Publications, **62,** 159-162.

MACDONALD, D.I.M., ARCHER, B., MURRAY, S., SMITH, K., BATES, A. 2007. Modelling and comparing the Caledonian and Permo-Triassic erosion surfaces across Highland Scotland: implications for landscape inheritance. *In:* NICHOLS, G., WILLIAMS, E. & PAOLA, C. (eds) *Sedimentary Processes, Environments and Basins: A Tribute to Peter Friend.* Special Publications of the IAS, **38,** 283-299.

MAGARA, K. 1976. Thickness of removed sedimentary rocks, palaeopore pressure and palaeotemperature, south-western part of Western Canada Basin. *AAPG Bulletin,* **60,** 554-565.

MARIE, J.P.P. 1975. Rotliegendes stratigraphy and diagenesis. *In:* WOODLAND, A.W. (ed.) *Petroleum and the Continental Shelf of North-west Europe, Volume 1, Geology,* Applied Science Publishers, 205-211.

MORTON, N. 1987. Jurassic subsidence history in the Hebrides, N.W. Scotland. *Marine and Petroleum Geology,* **4,** 226-241.

NIELSEN, S.B., GALLAGHER, K., LEIGHTON, C., BALLING, N., SVENNINGSEN, L., HOLM JACOBSEN, B., THOMSEN, E., NIELSEN, O.B., HEILMANN-CLAUSEN, EGHOLM, D.L., SUMMERFIELD, M.A., RØNØ CLAUSEN, O., PIOTROWSKI, J.A., THORSEN, M.R., HUUSE, M., ABRAHAMSEN, N., KING, C. & LYKKE-ANDERSEN, H. 2009. The evolution of western Scandinavian topography: a review of Neogene uplift versus the ICE (isostasy-climate-erosion) hypothesis. *Journal of Geodynamics,* **47,** 72-95.

PERSANO, C., BARFORD, D.N., STUART, F.M. & BISHOP, P. 2007. Constraints on early Cenozoic underplating-driven uplift and denudation of western Scotland from low temperature thermochronometry. *Earth and Planetary Science Letters,* **263,** 404-419.

PRAEG, D., STOKER, M.S., SHANNON, P.M., CERAMICOLA, S., HJELSTUN, B., LABERG, J.S. & MATHIESEN, A. 2005. Episodic Cenozoic tectonism and the development of the NW European 'passive' continental margin. *Marine and Petroleum Geology*, **22,** 1007-1030.

ROBERTS, A.M. & YIELDING, G. 1991. Deformation around basin-margin faults in the North Sea/mid-Norway rift. *In:* ROBERTS, A.M., YIELDING. G. & FREEMAN, B. (eds) *The Geometry of Normal Faults.* Geological Society, London, Special Publications, **56,** 61-78.

ROBERTS, A.M. & HOLDSWORTH, R.E. 1999. Linking onshore and offshore structures: Mesozoic extension in the Scottish Highlands. *Journal of the Geological Society,* **156,** 1061-1064.

SANDIFORD, M., WALLACE, M. & COBLENTZ, D. 2004. Origin of the *in situ* stress field in south-eastern Australia. *Basin Research,* **16,** 325-338.

SHAW CHAMPION, M.E., WHITE, N.J., JONES, S.M. & LOVELL, J.P.B. 2008. Quantifying transient mantle convective uplift: an example from the Faroe-Shetland basin. *Tectonics,* **27,** TC1002, doi:10.1029/2007TC002106.

SHUSTER, D.L., FLOWERS, R.M. & FARLEY, K.A. 2006. The influence of natural radiation damage on helium diffusion kinetics in apatite. *Earth and Planetary Science Letters,* **249,** 148-161.

STOKER, M.S., HITCHEN, K. & GRAHAM, C.G. 1993. *United Kingdom Offshore Regional Report: the Geology of the Hebrides and West Shetland Shelves, and Adjacent Deep-Water Areas.* British Geological Survey. HMSO, London.

STOKER, M.S., HOLFORD, S.P., HILLIS, R.R., GREEN, P.F. & DUDDY, I.R. 2010. Cenozoic post-rift sedimentation off Northwest Britain: Recording the detritus of episodic uplift on a passive continental margin. *Geology,* **38.**

THOMSON, K., UNDERHILL, J.R., GREEN, P.F., BRAY, R.J. & GIBSON, H.J. 1999. Evidence from apatite fission-track analysis for the post-Devonian burial and exhumation history of the northern Highlands, Scotland. *Marine and Petroleum Geology,* **16,** 27-39.

TURNER, J.P., GREEN, P.F., HOLFORD, S.P. & LAWRENCE, S. 2008. Thermal history of the obliquely divergent Rio Muni (West Africa)-NE Brazil margins during continental breakup. *Earth and Planetary Science Letters,* **270,** 354-367.

UNDERHILL, J. R. 1991. Implications of Mesozoic Recent basin development in the western lnner Moray Firth, UK. *Marine & Petroleum Geology,* **8,** 359 369.

UNDERHILL, J.R. 2001. Controls on the genesis and prospectivity of Paleogene palaeogeomorphic traps, East Shetland Platform, UK North Sea. *Marine and Petroleum Geology,* **18,** 259-281.

UNDERHILL, J.R. & PARTINGTON, M.A. 1993. Jurassic thermal doming and deflation in the North Sea: implications of the sequence stratigraphic evidence. *In:* PARKER, J.R. (ed.)

Petroleum Geology of Northwest Europe: Proceedings of the 4th Conference. Geological Society, London, 337-345.

UNDERHILL, J.R., MONAGHAN, A.A. & BROWNE, M.A.E. 2008. Controls on structural styles, basin development and petroleum prospectivity in the Midland Valley of Scotland. *Marine and Petroleum Geology*, **15,** 1000-1022.

WALKER, G.P.L. 1971. The distribution of amygdale minerals in Mull and Morven (Western Scotland). *In:* MURTY, T.V.V.G.G.R.K. & ROA, S.S. (eds) *Studies in Earth Sciences (W.D. West Commemoration Volume).* University of Saugur, India, 181-194.

WATSON, J. 1985. Northern Scotland as an Atlantic-North Sea divide. *Journal of the Geological Society, London,* **142,** 221-243.

WHITE, N. & LOVELL, B. 1997. Measuring the pulse of a plume with the sedimentary record. *Nature,* **387,** 888-891.

Figure captions

Fig. 1 Map of Scotland showing post-Ordovician geology and faults with evidence of post-Ordovician activity, and locations of samples used in this study (Fyfe et al., 1993; Stoker et al., 1993). Although Mesozoic and Cenozoic rocks are mainly restricted to the present-day offshore basins, sedimentary and volcanic outliers of Devonian, Carboniferous, Permian, Upper Triassic, Jurassic and Upper Cretaceous occur along the northwest coast. CB, Canna Basin; CF, Colonsay Fault; CL, Clisham; GGF, Great Glen Fault; HBF, Highland Boundary Fault; HF, Helmsdale Fault; HS, Hebrides Shelf; IMF, Inner Moray Firth; LMT, Little Minch Trough; M, Mull; MF, Minch Fault; NH, Northern Highlands; NMB, North Minch Basin; OH, Outer Hebrides; S, Skye; SD, Sgorr Dhonuill; SOHB, Sea of Hebrides Basin; SKF, Skerryvore Fault; STF, Strathconon Fault; WF, Wick Fault; WFB, West Flannan Basin; WLB, West Lewis Basin; WOB, West Orkney Basin; WSB, West Shetland Basin.

Fig. 2 Mean fission track ages plotted against mean track lengths for apatite fission track data used in this study, alongside previously published data from northwest Scotland (Lewis et al., 1992 (margins of Sea of Hebrides Basin); Thomson et al., 1999 (northern Highlands); Jolivet, 2007 (Loch Ness, Strontian); Persano et al., 2007 (Clisham, Sgorr Dhonuill)). All errors shown at ±1σ. Most fission track ages are younger than 300 Ma, suggesting these samples reached late Palaeozoic-Mesozoic palaeotemperatures sufficient to produce severe age reduction (i.e. >100°C). Ages from Skye and Mull mostly range between 50-70 Ma, similar to the timing of igneous activity in these regions, and suggesting that related thermal effects heavily influence fission track data from these regions. A typical 'boomerang trend' based on AFTA data from the Lake District (Green, 1986) is shown in the background.

Fig. 3 Comparison of the timing information derived from all AFTA data that show evidence for higher palaeotemperatures post-deposition/intrusion/metamorphism. Synthesis of results identifies a number of discrete phases of cooling, indicated by the vertical bands. Open boxes and arrow indicate the range of stratigraphic ages for individual samples. Horizontal bands define range of timing for the onset of cooling derived from AFTA data in each sample within a 95% confidence interval. Note that for several samples from 202/19-1 the timing estimates for individual estimates show some overlap. Timing estimates have been shifted vertically where this is the case.

Fig. 4 AFTA results and thermal history reconstruction for exploration well 202/19-1. a) Left, fission-track ages; right, mean track lengths, both plotted against depth below kelly bushing. Black lines show increasing stratigraphic age with depth. Greyscale lines show the predicted patterns of fission-track age and mean track length from the DTH for apatites containing 0.0-0.1, 0.4-0.5, 0.9-1.0 and1.5-1.6 wt% Cl. The DTH is based on the burial history derived from the sedimentary section intersected by the well, combined with the present-day geothermal gradient of 25.3°C km^{-1} determined from corrected BHT values in this well. The fission-track ages decrease with depth and are much less than the values predicted from the DTH, indicating that the sampled sedimentary units have been hotter in the past. b) Palaeotemperature constraints from AFTA data plotted against depth. AFTA data define two separate phases of cooling that have affected the preserved Permian-Triassic succession that began during the early Cretaceous (110 to 90 Ma) and Cenozoic (55 to 10 Ma). c) Ranges of amounts of removed section and palaeogeothermal gradients (hyperbolic ellipsoids) required to explain the early Cretaceous and Cenozoic palaeotemperatures. The hyperbolic ellipsoids define the parameter ranges estimated from AFTA that are consistent with the respective palaeotemperature constraints within 95% confidence limits. Black dots indicate the corresponding maximum likelihood solutions. Horizontal shaded band shows amount of removed section independently estimated from sonic velocity data (Evans, 1997).

Fig. 5 AFTA results and thermal history reconstruction for exploration well 134/5-1. a) Left, fission-track ages; right, mean track lengths, both plotted against depth below kelly bushing. Black lines show increasing stratigraphic age with depth. Greyscale lines show predicted patterns of fission-track age and mean track length from the DTH based on the preserved sedimentary section for apatites containing 0.0-0.1, 0.4-0.5, 0.9-1.0 and1.5-1.6 wt% Cl. The DTH for this well has been determined using the revised geothermal gradient of 43°C km^{-1} that is with AFTA data. b) Palaeotemperature constraints from AFTA and vitrinite reflectance (VR) data plotted against depth. AFTA and VR data define two episodes of Cenozoic cooling. Samples recording early Cenozoic (~60 Ma) palaeotemperatures are closely associated with coeval igneous intrusions and define no linear trend with depth, suggesting that cooling occurred following the cessation of contact and hydrothermal heating associated with igneous activity. Samples recording mid-Cenozoic (45 to 20 Ma) palaeotemperatures define a linear profile with depth which has a similar gradient to that of the present-day temperature profile. (c) Mid-Cenozoic cooling in these samples is explained by removal of ~0.6 to 0.9 km of post-Lower Jurassic section during a denudation episode which began between 45 and 20 Ma, for a palaeogeothermal gradient equal to the revised present-day value of 43°C km^{-1}.

Fig. 6 Post-400 Ma event diagram for northwest Scotland, comparing generalized stratigraphy with AFTA-constrained cooling episodes defined in this study and in the western British Isles (Holford et al., 2009a).

Fig. 7 Palaeotemperatures across northwest Scotland in each of the regional palaeothermal episodes defined in this study. a) Triassic (220-195 Ma in the Outer Hebrides and 245-225 Ma in Morvern and central Scotland). Lighter shading shows surface/seafloor outcrops of Permian-Triassic rocks, darker shading shows outcrops of Jurassic rocks. b) Early Cretaceous (110-90 Ma in the West Orkney Basin and 140-130 Ma in the Hebridean region). Lighter shading shows surface/seafloor outcrops of Permian-Triassic rocks, darker shading shows outcrops of Jurassic rocks. c) Early Palaeogene (65-60 Ma in Skye, Mull and Morvern, 75-40 Ma in the Hebridean region). Diagonal shading shows seafloor outcrops of Cenozoic sedimentary rocks, hatched shading shows surface/seafloor outcrops of Palaeogene igneous extrusive rocks, grey shading shows surface/seafloor outcrops of Palaeogene intrusive rocks. d) Mid-late Cenozoic (30-15 Ma in West Orkney Basin, 15-10 Ma in Hebridean region, 40-25 Ma in 134/5-1 and 20-10 Ma in Skye, Mull and Morvern).

Fig. 8 Mid-late Cenozoic exhumation estimates across northwest Scotland based on AFTA data. a) Estimates based on mid-point temperature for each sample, assuming a surface temperature of 10°C and a geothermal gradient that decreases linearly from 43°C km^{-1} at 134/5-1 to 25.3°C km^{-1} at 202/19-1. b) Horizontal bars represent the range of gross exhumation for each sample location (reflecting the range of palaeotemperatures estimated from AFTA), and thickness of Quaternary deposits (i.e. post-exhumation reburial). Adding the thickness of Quaternary sediments to the gross estimates gives an estimate of net exhumation for each location. Results indicate that large areas of northwest Scotland and its offshore basins have had >0.5-1.0 km of section removed during late Cenozoic exhumation.

Fig. 9 AFTA data from the Morvern peninsula. a) Geological map of the Morvern peninsula. b) Thermal histories for AFTA samples from various stratigraphic levels. Results indicate exhumation of basement rocks to surface levels by the late Triassic, following which they were reheated during late-Triassic-Jurassic burial, and then cooled through several stages of Cretaceous-Cenozoic exhumation. c) Schematic post-400 Ma thermal history of the Morvern peninsula reconciling results from all AFTA samples.

Fig. 10 Schematic ~E-W cross-sections illustrating our preferred model for the post-Caledonian geological evolution of northwest Scotland. (a) Early Devonian post-orogenic uplift witnessed by the unroofing of the Newer Granites (Watson, 1985; Hall, 1991). (b) Devonian extensional collapse and subsidence permitting deposition of >2-3 km of Devonian and Lower Carboniferous rocks (Thomson et al., 1999). (c) Late Carboniferous deformation and uplift related to far-field Variscan compression (Underhill et al., 2008) removing Devonian and Carboniferous sediments. (d) Late Triassic-Jurassic extension and subsidence leading to formation of Hebridean basins (Fyfe et al., 1993) but also affecting pre-Caledonian basement rocks (Roberts & Holdsworth, 1999). Localised uplift in footwalls of major faults, and regional uplift of basement rocks in western and central Scotland. Maximum post-Caledonian burial depths across northwest Scotland are attained during the late Jurassic-early Cretaceous with up to 2-3 km of subsequently eroded syn and post-rift Jurassic rocks deposited across this region. (e) Early Cretaceous regional uplift and exhumation beginning ~120 Ma followed by late Cretaceous sea level rises permitting Chalk deposition (f). (g) Localised early Cenozoic uplift (beginning ~65-60 Ma) around Palaeogene igneous intrusive centres. Considerable thicknesses of lavas accumulate in some areas (e.g. around Mull), much of which are eroded during later exhumation. (h) Regional exhumation beginning during the mid-Cenozoic (40-25 Ma) and late Cenozoic (15-0 Ma) removing up to 1.9 km of overburden, followed by Pliocene-Pleistocene uplift not directly constrained by our AFTA data but witnessed by shelf-slope wedges of clastic sediment that prograde away from northwest Scotland (Stoker et al., 1993).

Table 1 Apatite fission track analysis sample details.

Table 2 Summary of palaeotemperatures analysis and Default Thermal History interpretations.

Holford et al Figure 1

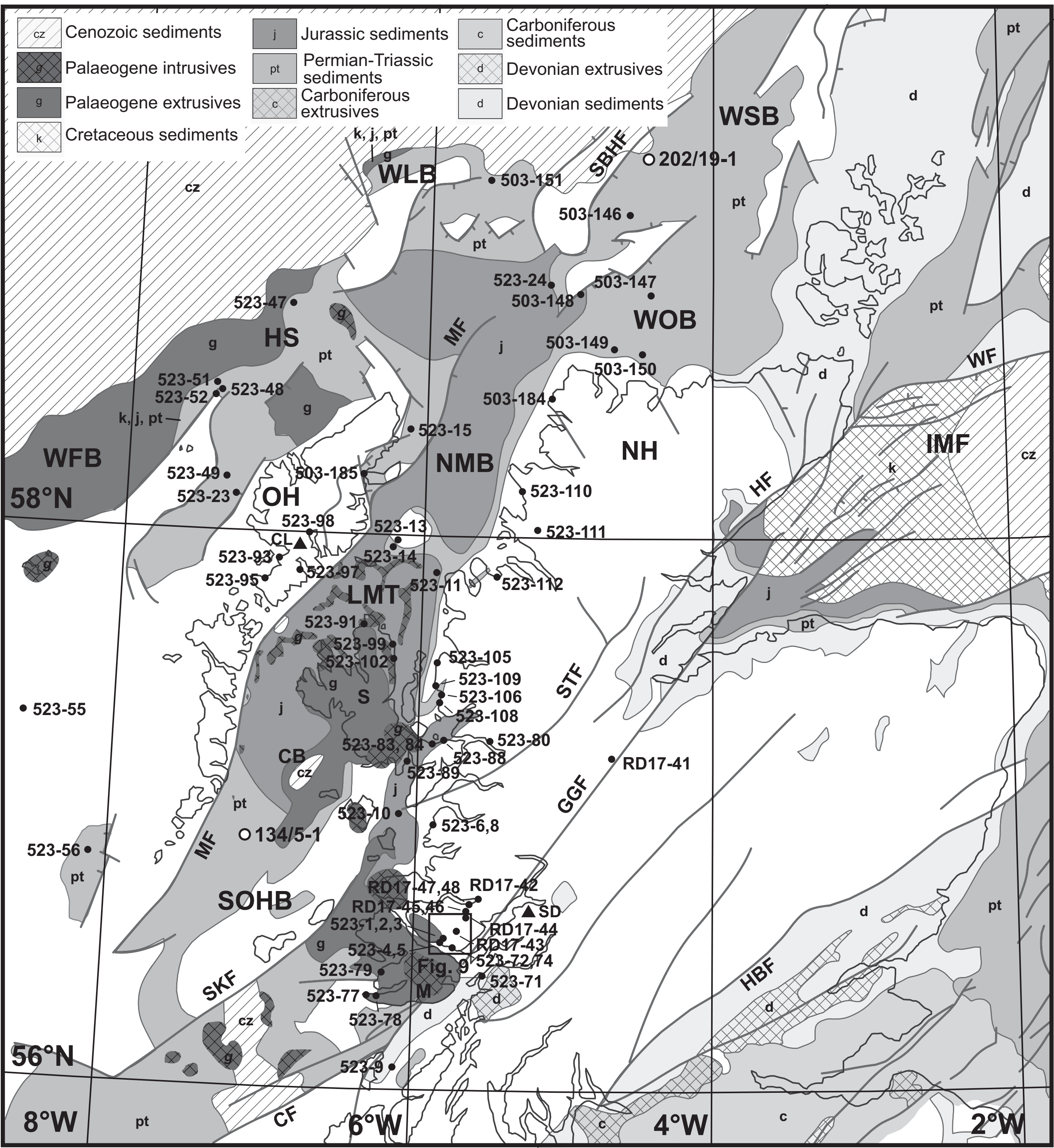

Holford et al Figure 2

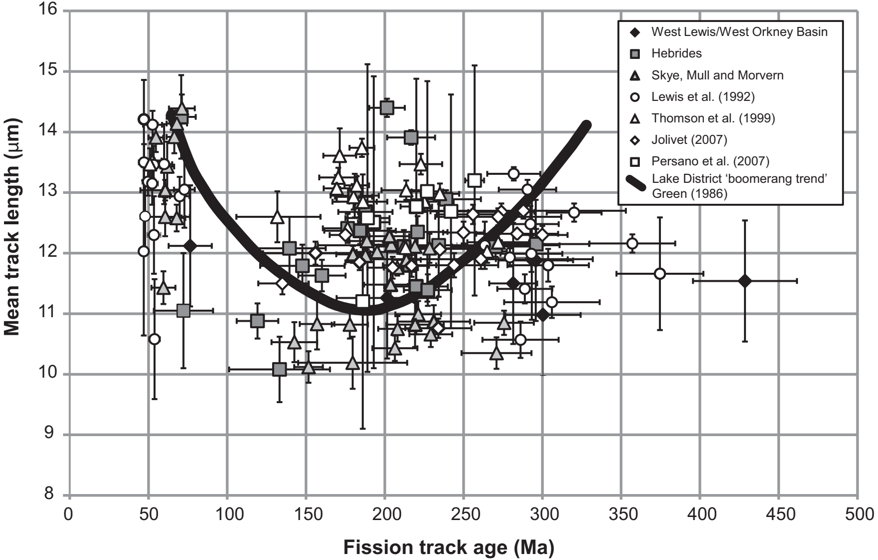

Holford et al Figure 3

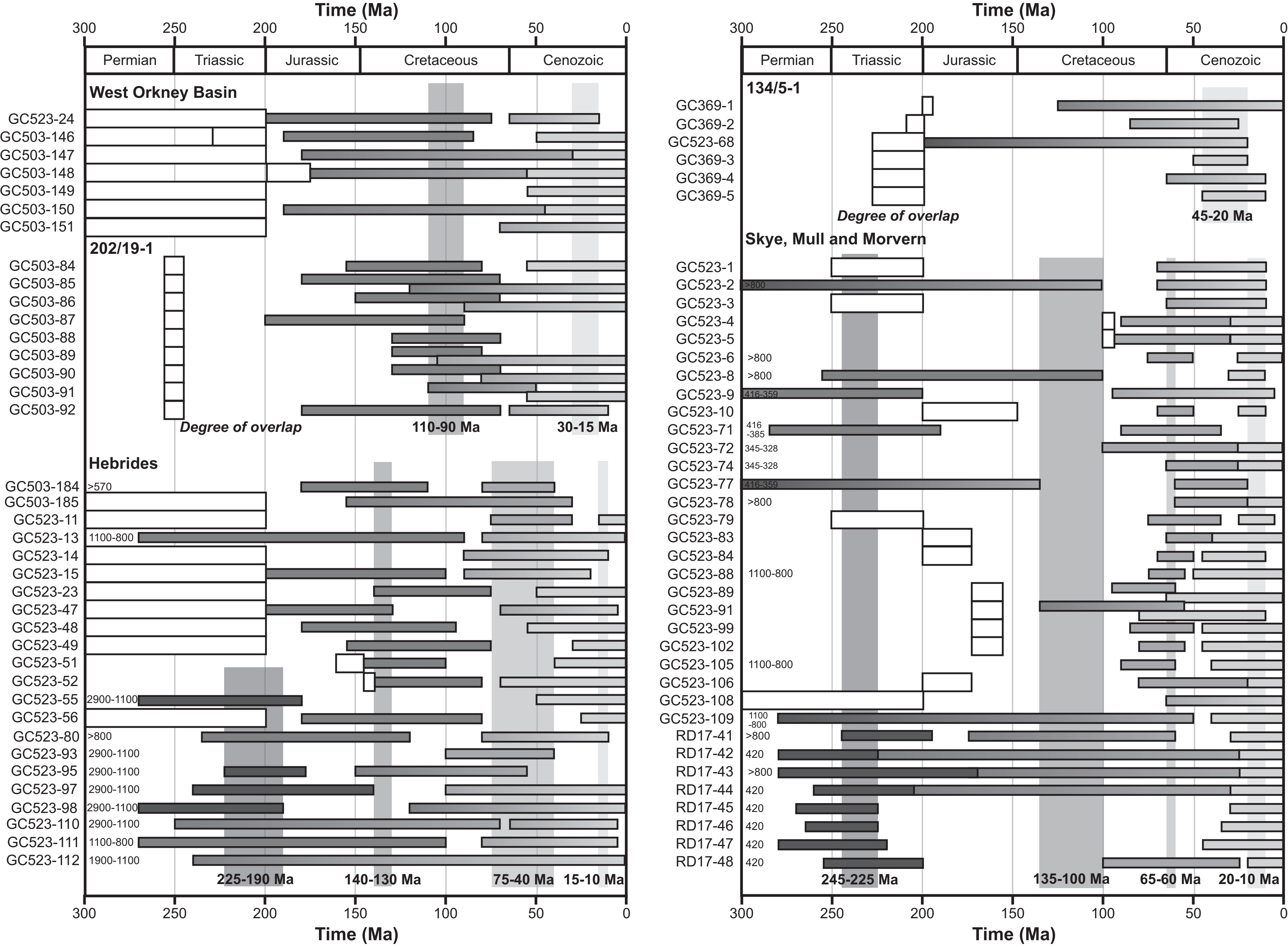

Holford et al Figure 4

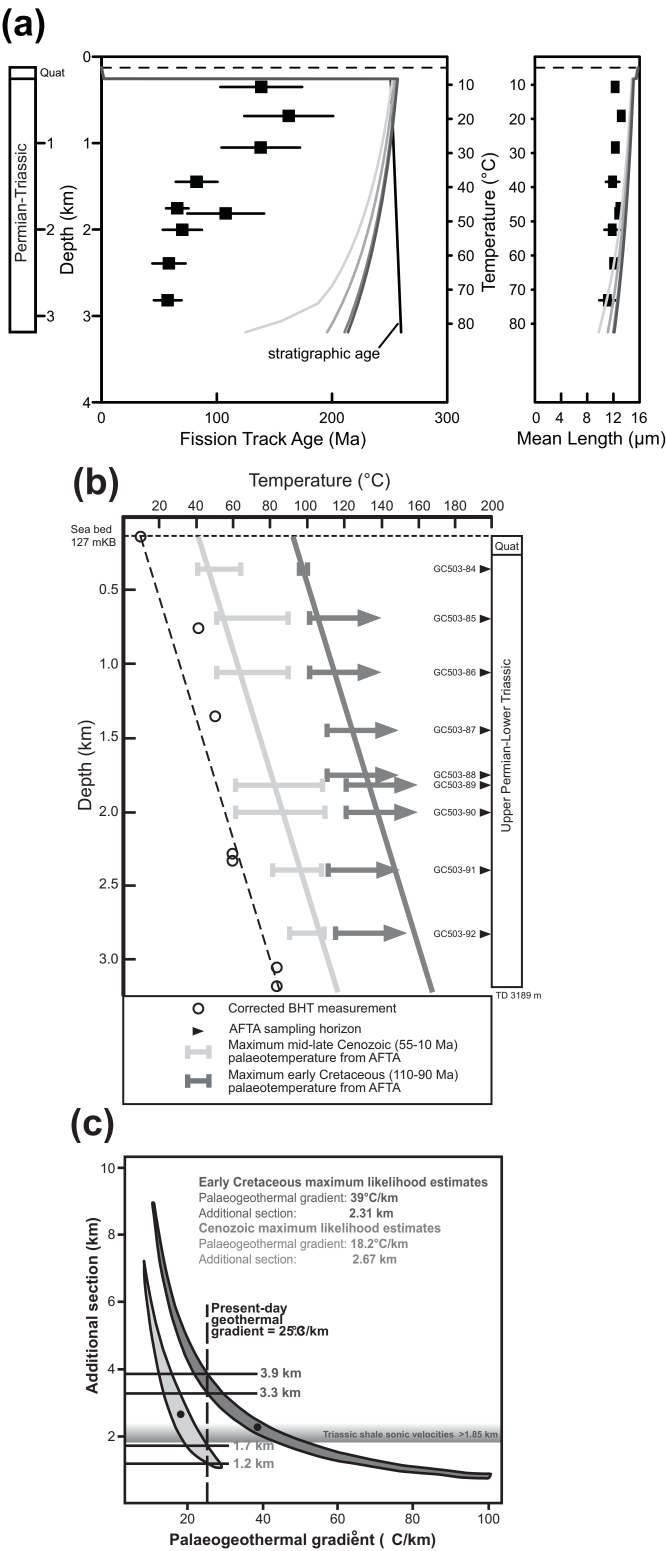

Holford et al Figure 5

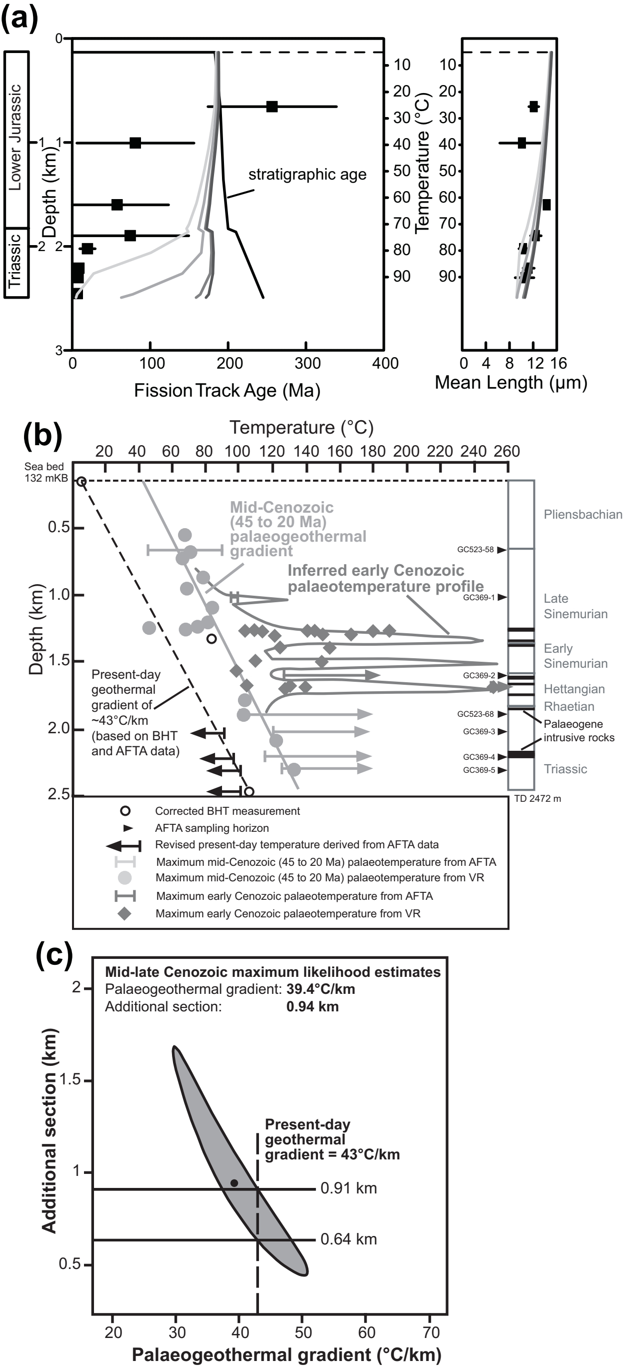

Holford et al Figure 6

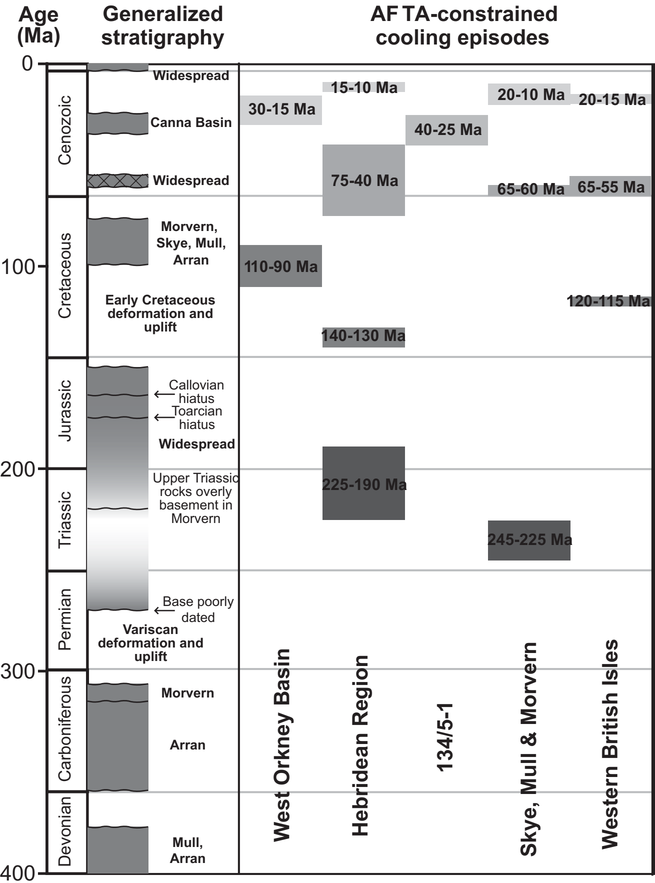

Holford et al Figure 7

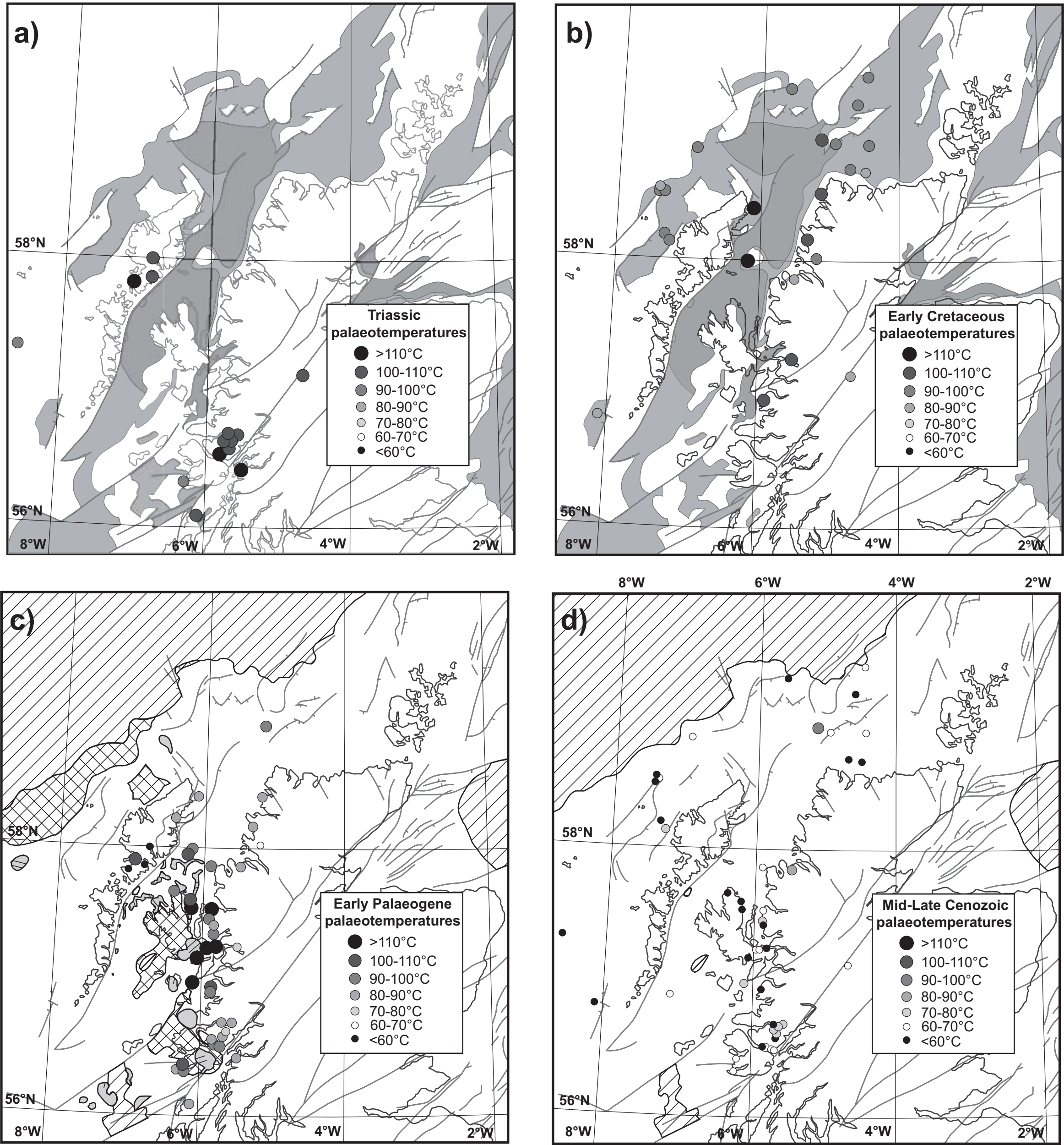

Holford et al Figure 8

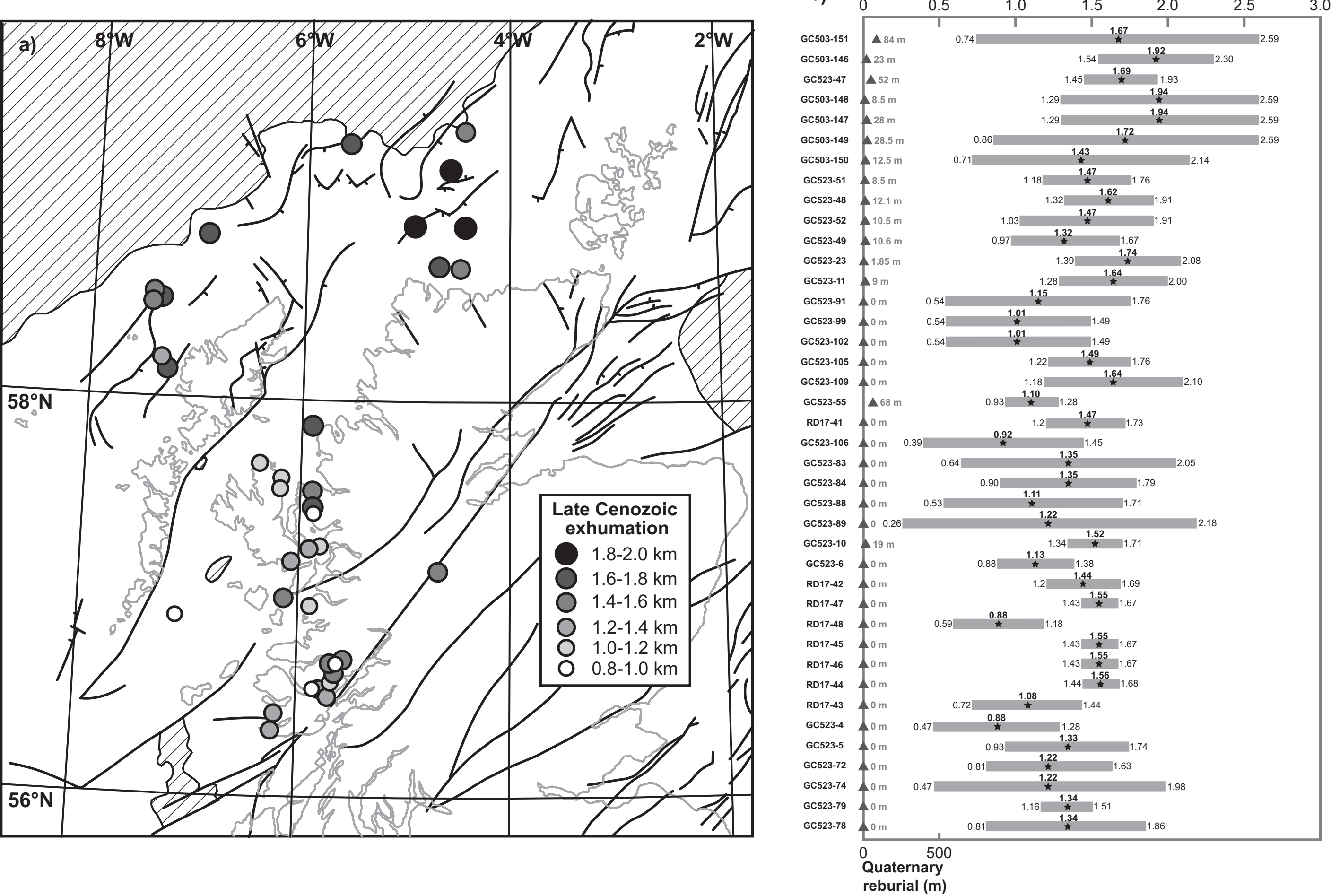

Holford et al Figure 9

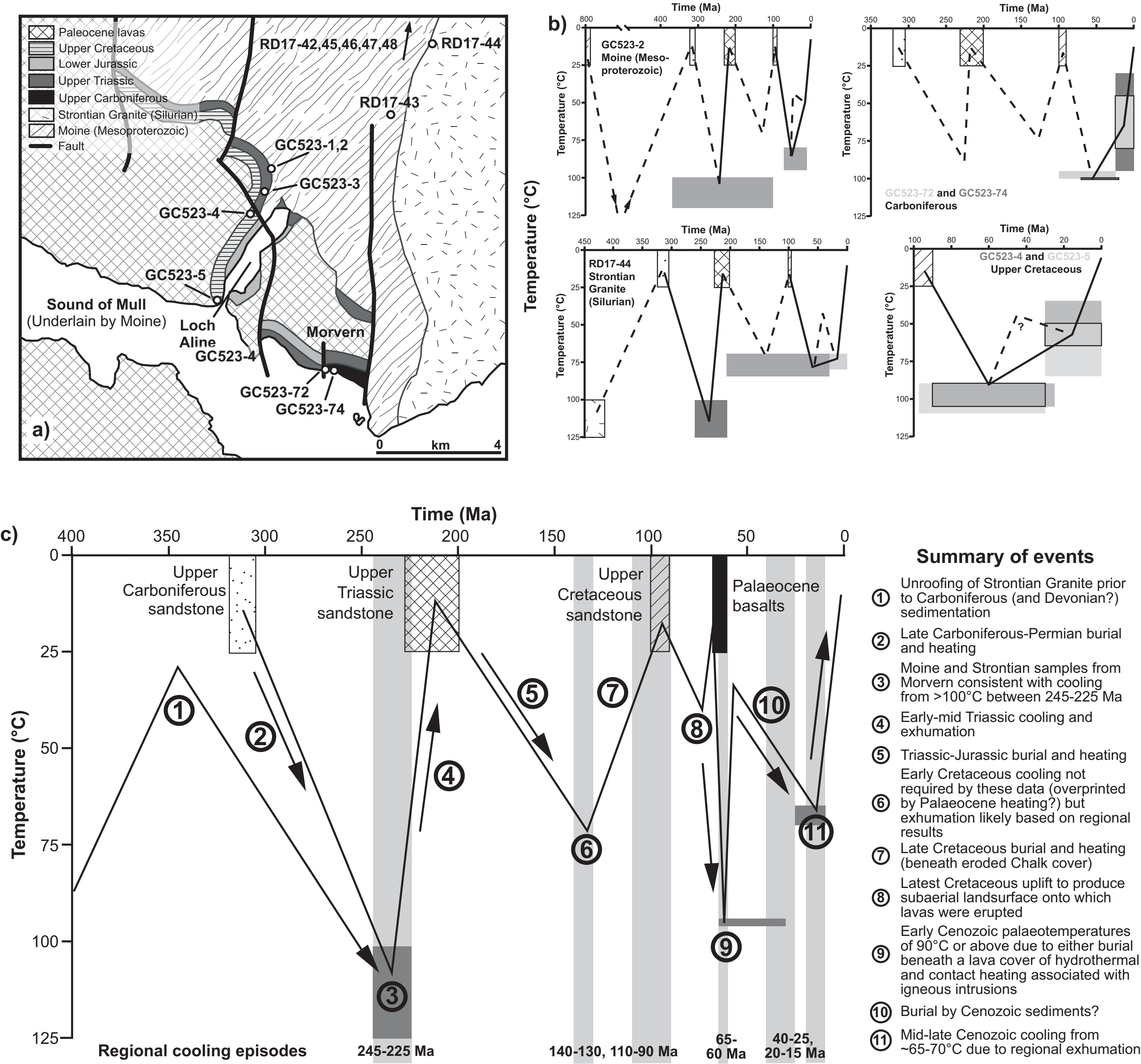

Holford et al Figure 10

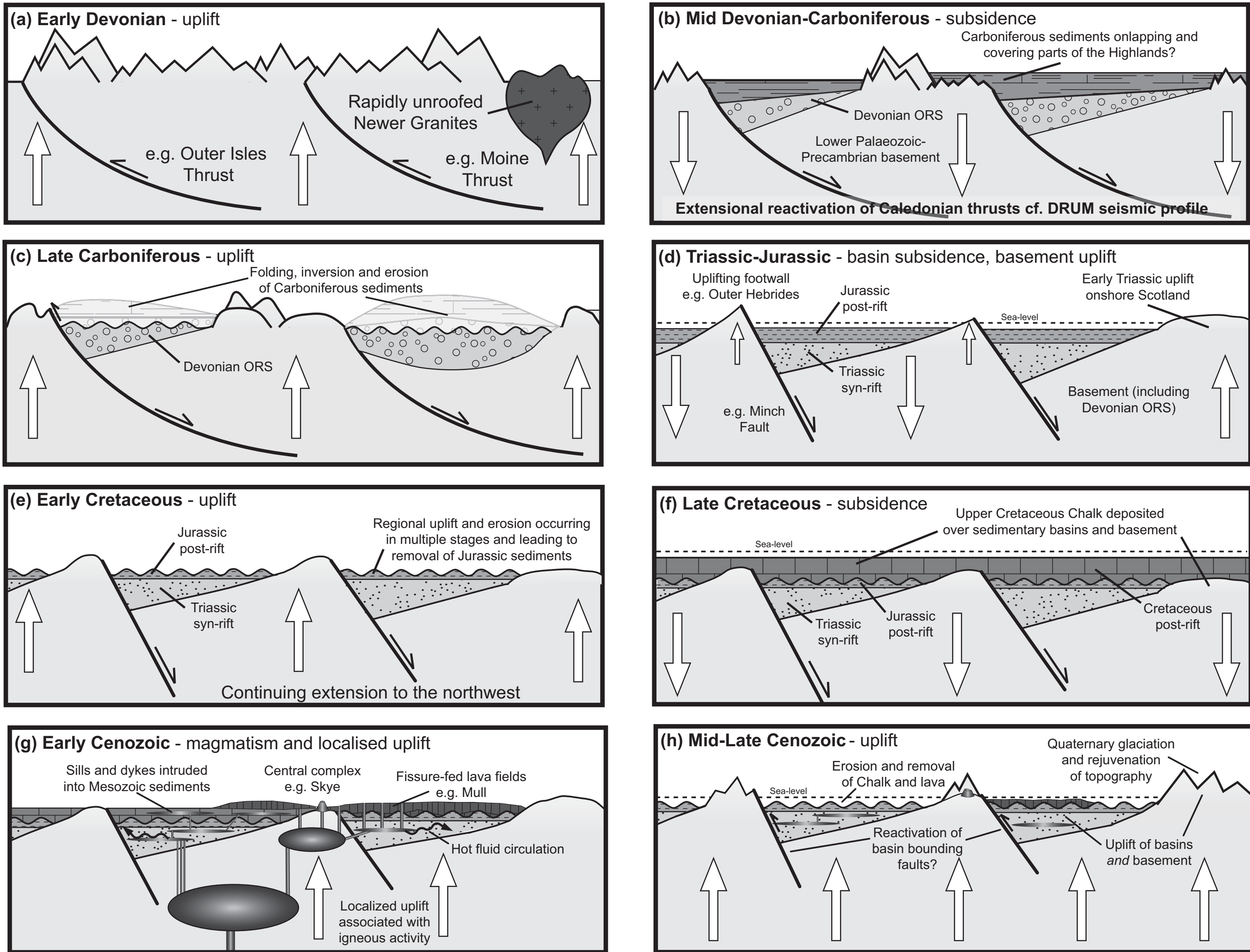

Sample number	Sample location (depth bsl if offshore)	Stratigraphic age (Ma)	Uranium content (ppm)	Fission track age (Ma ± 1σ)[a]	$P[\chi^2]$ (number of grains)	Mean track length (µm)	S.D. (µm) (number of track lengths)
West Orkney Basin							
GC523-24	BGS rockdrill 58-06/642 (4.7 m)	Permian-Triassic (299-200)	4	76.5 ± 13.7	17 (20)	12.12 ± 0.60	2.55 (18)
GC503-146	BGS BH72/37 (9-21 m)	Triassic (251-200)	17	239.3 ± 22.8	<1 (19)	11.90 ± 0.19	1.87 (100)
GC503-147	BGS BH73/31 (28-31 m)	Permian-Triassic (299-200)	9	300.4 ± 23.9	<1 (20)	10.98 ± 0.20	2.04 (100)
GC503-148	BGS BH72/34 (14 m)	Lower Jurassic (200-176)	12	201.5 ± 32.1	<1 (12)	11.26 ± 0.35	2.48 (51)
GC503-149	BGS BH73/29 (31-36 m)	Permian-Triassic (299-200)	13	281.5 ± 15.2	14 (20)	11.50 ± 0.17	1.83 (118)
GC503-150	BGS BH72/25 (15-19m)	Permian-Triassic (299-200)	10	295.8 ± 23.7	<1 (20)	11.88 ± 0.17	1.74 (101)
GC503-151	BGS BH78/07 (125-128 m)	Permian-Triassic (299-200)	10	428.6 ± 33.0	<1 (20)	11.54 ± 0.18	1.84 (109)
202/19-1							
GC503-84	274-427 m	Upper Permian (260-251)	22	138.6 ± 17.7	<1 (20)	12.27 ± 0.23	2.00 (75)
GC503-85	610-762 m	Upper Permian (260-251)	13	162.5 ± 19.3	<1 (20)	13.21 ± 0.19	1.77 (84)
GC503-86	975-1128 m	Upper Permian (260-251)	15	138.1 ± 17.0	<1 (20)	12.30 ± 0.28	2.11 (57)
GC503-87	1372-1524 m	Upper Permian (260-251)	10	82.5 ± 9.1	6 (20)	11.88 ± 0.51	1.52 (9)
GC503-88	1753-1758 m	Upper Permian (260-251)	28	65.8 ± 4.9	5 (20)	12.99 ± 0.16	1.23 (56)
GC503-89	1810-1819 m	Upper Permian (260-251)	23	107.8 ± 16.6	<1 (20)	12.81 ± 0.33	1.58 (23)
GC503-90	1999-2008 m	Upper Permian (260-251)	17	70.1 ± 8.5	93 (20)	11.82 ± 0.60	1.88 (10)
GC503-91	2316-2469 m	Upper Permian (260-251)	26	58.5 ± 7.2	<1 (20)	12.03 ± 0.31	1.60 (27)
GC503-92	2743-2895 m	Upper Permian (260-251)	21	57.4 ± 6.0	<1 (20)	11.08 ± 0.62	2.24 (13)
Hebrides							
GC503-184	Balchrick	Torridonian (1000-530)	24	176.4 ± 15.7	<1 (20)	12.41 ± 0.24	2.36 (100)
GC503-185	Tolm, Lewis	Permian-Triassic (299-200)	20	212.1 ± 16.0	<1 (20)	12.11 ± 0.28	2.10 (58)
GC523-11	BGS BH71/11 (19-25 m)	Permian-Triassic (299-200)	12	119.2 ± 13.2	<1 (20)	10.88 ± 0.29	2.65 (82)
GC523-13	BGS BH71/13 (14.5-15 m)	Torridonian (1000-530)	15	133.2 ± 32.0	<1 (15)	10.08 ± 0.54	2.21 (17)
GC523-14	BGS BH71/14 (23-27 m)	Permian-Triassic (299-200)	11	72.2 ± 18.8	<1 (13)	11.05 ± 0.95	3.16 (11)
GC523-15	BGS BH72/32 (28-36 m)	Permian-Triassic (299-200)	8	139.5 ± 23.0	4 (13)	12.08 ± 0.52	2.50 (23)
GC523-23	BGS rockdrill 58-08/94 (1.85-2.6 m)	Permian-Triassic (299-200)	17	160.1 ± 15.0	<1 (19)	11.63 ± 0.26	2.68 (106)
GC523-47	BGS BH78/05 (54 m)	Permian-Triassic (299-200)	7	187.7 ± 17.2	13 (20)	12.68 ± 0.19	1.93 (104)
GC523-48	BGS BH88/04 (11.15-12.61 m)	Permian-Triassic (299-200)	11	184.3 ± 22.7	<1 (20)	12.37 ± 0.22	2.30 (106)
GC523-49	BGS BH88/08 (11.5-12.1 m)	Permian-Triassic (299-200)	13	219.8 ± 20.2	3 (20)	11.45 ± 0.27	2.75 (106)
GC523-51	BGS BH90/08 (17.25-12 m)	Upper Jurassic (161-145)	27	270.3 ± 27.5	<1 (20)	12.11 ± 0.17	1.91 (125)
GC523-52	BGS BH90/09 (18-22.3 m)	Lower Cretaceous (145-100)	7	220.8 ± 19.0	71 (20)	12.35 ± 0.26	1.52 (34)
GC523-55	BGS BH90/14 (91 m)	Lewisian (>2500)	18	238.9 ± 22.1	<1 (20)	12.89 ± 0.15	1.65 (114)
GC523-56	BGS BH90/16 (75-76.5 m)	Permian-Triassic (299-200)	9	215.7 ± 16.9	7 (20)	11.80 ± 0.31	2.40 (62)
GC523-80	Dornie, Loch Duich	Moine (1100-800)	15	227.3 ± 15.2	21 (20)	11.39 ± 0.26	2.68 (106)
GC523-93	Luskentyre, Harris	Lewisian (>2500)	4	70.8 ± 9.2	17 (20)	14.25 ± 0.69	1.70 (6)
GC523-95	Northton, Harris	Lewisian (>2500)	11	201.4 ± 11.3	22 (20)	14.40 ± 0.15	1.48 (102)
GC523-97	Meavag, Harris	Lewisian (>2500)	4	180.9 ± 15.3	70 (20)	12.95 ± 0.36	2.13 (35)
GC523-98	Bowglass, Harris	Lewisian (>2500)	6	216.7 ± 15.2	17 (20)	13.91 ± 0.12	1.26 (111)
GC523-110	Achmelvich Bay	Lewisian (>2500)	2	147.7 ± 26.8	75 (20)	11.79 ± 0.35	2.37 (46)
GC523-111	Loch Lurgainn	Torridonian (1000-530)	18	296.1 ± 33.6	<1 (7)	12.15 ± 0.25	2.20 (77)
GC523-112	Gruinard Bay	Lewisian (>2500)	1	234.2 ± 76.7	89 (20)	12.13 ± 0.85	1.90 (5)
134/5-1							
GC523-58	579-731 m	Pliensbachian (190-183)	13	256.7 ± 41.3	9 (5)	12.11 ± 0.42	0.84 (4)
GC369-1	930-1082 m	Sinemurian (197-190)	26	81.1 ± 37.6	<1 (5)	10.11 ± 1.88	4.20 (5)
GC369-2	1524-1676 m	Hettangian-Sinemurian (200-190)	16	57.7 ± 33.0	<1 (4)	14.30 ± 0.27	0.38 (2)
GC523-68	1829-1966 m	Triassic (251-200)	9	74.5 ± 37.5	<1 (8)	12.46 ± 0.45	1.09 (6)
GC369-3	1966-2079 m	Triassic (251-200)	16	19.6 ± 4.9	<1 (19)	10.30 ± 0.35	1.88 (29)
GC369-4	2164-2255 m	Triassic (251-200)	33	8.7 ± 2.1	<1 (22)	11.24 ± 0.47	1.04 (5)
GC369-5	2255-2347 m	Triassic (251-200)	32	7.6 ± 0.8	14 (20)	10.54 ± 0.79	3.06 (15)

Skye, Mull and Morvern							
GC523-1	Loch Aline, Morvern	Triassic (251-200)	18	229.2 ± 13.6	63 (20)	10.66 ± 0.21	2.13 (102)
GC523-2	Loch Aline, Morvern	Moine (1100-800)	18	206.4 ± 14.3	52 (20)	10.43 ± 0.21	2.25 (110)
GC523-3	Loch Aline, Morvern	Triassic (251-200)	18	208.1 ± 12.3	69 (20)	10.75 ± 0.21	2.17 (107)
GC523-4	Loch Aline, Morvern	Cenomanian (100-94)	21	221.2 ± 14.5	79 (20)	10.99 ± 0.22	2.18 (102)
GC523-5	Loch Aline, Morvern	Cenomanian (100-94)	15	219.2 ± 18.2	<1 (17)	10.82 ± 0.37	2.19 (35)
GC523-6	Glenancross	Moine (1100-800)	8	59.5 ± 7.6	98 (20)	11.43 ± 0.27	2.70 (103)
GC523-8	Glenancross	Moine (1100-800)	15	177.8 ± 11.5	21 (20)	10.82 ± 0.23	2.29 (103)
GC523-9	BGS BH71/09 (42-46 m)	Devonian (416-359)	5	231.1 ± 23.0	23 (20)	10.87 ± 0.27	2.01 (57)
GC523-10	BGS BH71/10 (20-22 m)	Jurassic (200-145)	26	60.6 ± 15.7	<1 (14)	13.04 ± 0.17	1.83 (115)
GC523-71	Ganavan Bay	Lower-Middle Devonian (416-385)	11	228.4 ± 26.5	<1 (19)	12.08 ± 0.24	2.30 (88)
GC523-72	Inninmore Bay, Morvern	Visean (345-328)	13	157.0 ± 11.0	33 (20)	10.83 ± 0.42	2.80 (44)
GC523-74	Inninmore Bay, Morvern	Visean (345-328)	10	142.6 ± 14.5	<1 (20)	10.53 ± 0.33	3.44 (108)
GC523-77	Fionnphort, Mull	Devonian (416-359)	7	203.7 ± 16.9	9 (20)	11.48 ± 0.22	2.20 (101)
GC523-78	Bunessan, Mull	Moine (1100-800)	24	151.6 ± 9.1	28 (20)	10.12 ± 0.26	2.75 (110)
GC523-79	Balnahard, Mull	Triassic (251-200)	11	67.9 ± 5.5	20 (20)	12.58 ± 0.22	2.27 (102)
GC523-83	Broadford Bay, Skye	Lower Jurassic (200-176)	21	52.3 ± 6.0	<1 (20)	13.53 ± 0.29	1.66 (32)
GC523-84	Broadford Bay, Skye	Lower Jurassic (200-176)	16	54.7 ± 4.7	3 (20)	13.91 ± 0.24	1.53 (40)
GC523-88	Drocaid Lusa, Skye	Torridonian (1000-530)	23	61.9 ± 4.4	19 (20)	13.43 ± 0.41	2.20 (29)
GC523-89	Loch Slapin, Skye	Middle Jurassic (176-161)	12	71.2 ± 8.2	<1 (20)	14.39 ± 0.23	1.55 (45)
GC523-91	Cairidh Ghlumaig, Skye	Middle Jurassic (176-161)	13	219.2 ± 18.4	<1 (20)	12.11 ± 0.30	2.53 (72)
GC523-99	Staffin, Skye	Middle Jurassic (176-161)	22	66.4 ± 4.9	9 (20)	13.92 ± 0.27	0.99 (13)
GC523-102	Culnacnoc, Skye	Middle Jurassic (176-161)	19	68.0 ± 6.5	<1 (20)	14.14 ± 0.18	1.12 (39)
GC523-105	Cuaig	Torridonian (1000-530)	26	60.6 ± 15.7	<1 (14)	12.60 ± 0.32	2.44 (60)
GC523-106	Applecross	Lower Jurassic (200-176)	13	275.7 ± 18.9	8 (19)	10.85 ± 0.20	2.11 (108)
GC523-108	Applecross	Permian-Triassic (299-200)	16	179.6 ± 34.6	<1 (10)	10.19 ± 0.43	2.21 (27)
GC523-109	Applecross	Torridonian (1000-530)	13	270.9 ± 22.2	4 (20)	10.35 ± 0.26	2.69 (108)
RD17-41	Fort Augustus	Moine (1100-800)	29	179.8 ±10.6	<1 (20)	11.98 ± 0.14	1.41 (104)
RD17-42	Strontian (A884)	Strontian Granite (420)	37	207.9 ± 8.5	96 (20)	11.76 ± 0.13	1.43 (120)
RD17-43	Coire nam Muc (A884)	Moine (1100-800)	36	213.7 ± 9.1	23 (20)	11.89 ± 0.14	1.48 (109)
RD17-44	Beinn Chlaonleud (A884)	Strontian Granite (420)	32	187.7 ± 9.2	10 (20)	11.96 ± 0.11	1.13 (100)
RD17-45	Beathrach (A884)	Strontian Granite (420)	32	195.1 ± 13.0	<1 (20)	12.02 ± 0.11	1.08 (102)
RD17-46	Beathrach (A884)	Strontian Granite (420)	32	204.1 ± 12.3	<1 (20)	12.14 ± 0.12	1.28 (108)
RD17-47	Liddesdale (A884)	Strontian Granite (420)	30	202.9 ± 12.6	<1 (20)	12.28 ± 0.13	1.27 (101)
RD17-48	Liddesdale (A884)	Strontian Granite (420)	28	188.6 ± 11.1	<1 (20)	12.02 ± 0.14	1.40 (100)

Table 1. Apatite fission track analysis sample details

[a]Central age (Galbraith and Laslett, 1993) used for samples containing a significant spread in single grain ages (P[χ^2]>5%), otherwise the "pooled age" is quoted. All ages were calculated using the zeta calibration approach of Hurford and Green (1983) using zeta values of 336.0±6.0 for samples GC369-1 to 5 (SRM612 dosimeter glass), 380.4±5.7 for samples GC503-84 to 92 (CN5 dosimeter glass), 354.8±6.3 for GC503-184 and 185 (SRM612), 386.9±6.9 for GC523-88 to 102 (CN5), 378.4±5.5 for GC503-146 to 151 (CN5), 392.9±7.4 for GC523-1 to 84 and GC523-105-112 (CN5), 348.8±5.2 for RD17-41 and 44-48 (SRM612) and 360.3±6.8 for RD17-42 and 43 (SRM612). All errors quoted at ±1σ. All analytical details are as described by Green et al. (2001), with the exception that the thermal neutron irradiation showed a significant flux gradient, and the appropriate value of ρD was determined by linear interpolation through the stack of grain mounts.

Sample number	Predicted FTA from DTH (Ma); measured FTA (Ma)	Predicted MTL from DTH (µm); measured MTL (µm)	Cooling episodes							
			Pre-Cretaceous		Cretaceous		Early Cenozoic		Mid-Late Cenozoic	
			Max. palaeotemperature (°C)	Onset of cooling (Ma)	Max. palaeotemperature (°C)	Onset of cooling (Ma)	Max. palaeotemperature (°C)	Onset of cooling (Ma)	Max. palaeotemperature (°C)	Onset of cooling (Ma)
West Orkney Basin										
GC523-24	208-290 (76.5)	14.7 (12.12)			≥105	200-75			90-100	65-15
GC503-146	146-210 (239.3)	14.7 (11.90)			85-95	190-185			50-70	50-0
GC503-147	208-290 (300.4)	14.7 (10.98)			85-95	180-130			45-80	30-0
GC503-148	178-208 (201.5)	14.7 (11.26)			90-100	185-55			45-80	55-0
GC503-149	208-290 (281.5)	14.7 (11.50)			85-110	≥45			35-85	55-0
GC503-150	208-290 (295.8)	14.7 (11.88)			80-90	190-45			30-70	45-0
GC503-151	208-290 (428.6)	14.7 (11.54)			80-105	≥50			30-80	70-0
202/19-1										
GC503-84	246 (138.6)	14.7 (12.27)			95-100	155-80			40-65	55-0
GC503-85	246 (162.5)	14.4 (13.21)			≥100	180-70			50-90	120-0
GC503-86	246 (138.1)	14.1 (12.30)			≥100	150-70			50-90	90-0
GC503-87	243 (82.5)	13.7 (11.88)			≥110	200-90				
GC503-88	238 (65.8)	13.2 (12.99)			≥110	130-70				
GC503-89	239 (107.8)	13.2 (12.81)			≥120	130-80			60-105	105-0
GC503-90	236 (70.1)	12.8 (11.82)			≥120	130-70			60-110	80-0
GC503-91	225 (58.5)	12.0 (12.03)			≥110	110-50			80-105	55-0
GC503-92	200 (57.4)	10.8 (11.08)			≥115	180-70			90-110	65-10
Overlap						**110-90 Ma**				**30-15 Ma**
Hebrides										
GC503-184	570 (176.4)	14.7 (12.41)			100-105	180-110	75-85	80-40		
GC503-185	208-290 (212.1)	14.7 (12.11)					75-90	155-30		
GC523-11	208-290 (119.2)	14.7 (10.88)					95-100	75-30	55-80	15-0
GC523-13	800-1100 (133.2)	14.7 (10.08)			115-125	270-90	90-100	80-0		
GC523-14	208-290 (72.2)	14.7 (11.05)					100-105	90-10		
GC523-15	208-290 (139.5)	14.7 (12.08)			105-115	200-100	80-95	90-20		
GC523-23	208-290 (160.1)	14.7 (11.63)			95-105	140-75			60-85	50-0
GC523-47	208-245 (187.7)	14.7 (12.68)			90-105	205-130			55-70	70-5
GC523-48	208-245 (184.3)	14.7 (12.37)			95-105	180-95			55-75	55-0
GC523-49	208-245 (219.8)	14.7 (11.45)			95-100	155-75			45-70	30-0
GC523-51	208-290 (270.3)	14.7 (12.11)			80-95	260-100			50-70	40-0
GC523-52	208-290 (220.8)	14.7 (14.51)			80-105	270-80			45-75	70-0
GC523-55	1100-2900 (238.9)	14.7 (12.89)	95-105	270-170					50-65	50-0
GC523-56	208-245 (215.7)	14.7 (11.80)			85-95	170-70			45-65	25-0
GC523-80	800 (227.3)	14.7 (11.39)			100-105	235-120	70-80	80-10		
GC523-93	1100-2900 (70.8)	14.7 (14.25)					100-110	100-40		
GC523-95	1100-2900 (201.4)	14.7 (14.40)	≥120	225-175			45-70	100-55		
GC523-97	1100-2900 (180.9)	14.7 (12.95)	105-110	240-140			45-75	100-0		
GC523-98	1100-2900 (216.7)	14.7 (13.91)	≥105	270-190			45-65	120-20		
GC523-110	1100-2900 (147.7)	14.7 (11.79)			100-110	250-70	75-90	65-5		
GC523-111	800-1100 (296.1)	14.7 (12.15)			90-100	270-100	50-75	80-5		
GC523-112	1100-1900 (234.2)	14.7 (12.13)			70-100	240-0	70-100	240-0	70-100	240-0
Overlap				**225-190 Ma**		**140-130 Ma**		**75-40 Ma**		**15-10 Ma**

134/5-1										
GC523-58	184 (256.7)	14.0 (12.11)							45-90	195-0
GC369-1	180 (81.1)	13.5 (10.11)					95-100	125-0		
GC369-2	167 (57.7)	12.7 (14.30)					≥125	85-25		
GC523-68	129 (74.5)	9.9 (12.46)							≥100	245-20
GC369-3	96 (19.6)	10.3 (10.30)							≥120	50-20
GC369-4	29 (8.7)	10.0 (11.24)							≥115	65-10
GC369-5	18 (7.6)	10.6 (10.54)							≥125	45-10
Overlap								**85-25 Ma**		**45-20 Ma**
Skye, Mull and Morvern										
GC523-1	208-290 (229.2)	14.7 (10.66)					85-90	70-10		
GC523-2	800 (206.4)	14.7 (10.43)	100-120	370-100			80-95	70-10		
GC523-3	208-290 (208.1)	14.7 (10.75)					80-90	65-10		
GC523-4	90-97 (221.2)	14.7 (10.99)					90-105	90-25	30-65	30-0
GC523-5	90-97 (219.2)	14.7 (10.82)					90-110	97-30	50-85	30-0
GC523-6	800 (59.5)	14.7 (11.43)					≥100	70-50	45-65	25-0
GC523-8	800 (177.8)	14.7 (10.82)			100-105	255-100	85-95	30-10		
GC523-9	363-403 (231.1)	14.7 (10.87)	≥100	400-210			85-95	95-5		
GC523-10	146-208 (60.6)	14.7 (13.04)					≥125	70-50	65-80	25-10
GC523-71	386-408 (228.4)	14.7 (12.08)	110-120	285-190			80-90	90-35		
GC523-72	333-350 (157.0)	14.7 (10.83)					95-100	100-25	45-80	25-0
GC523-74	333-350 (142.6)	14.7 (10.53)					100	70-20	30-95	25-0
GC523-77	363-408 (203.7)	14.7 (11.48)	95-105	305-135			80-90	60-20		
GC523-78	800 (151.6)	14.7 (10.12)					95-100	60-20	45-90	20-0
GC523-79	208-245 (67.9)	14.7 (12.58)					100-105	75-35	60-75	25-5
GC523-83	178-208 (52.3)	14.7 (13.53)					≥115	65-40	35-90	40-0
GC523-84	178-208 (54.7)	14.7 (13.91)					≥120	70-50	45-80	45-10
GC523-88	800-1100 (61.9)	14.7 (13.43)					≥110	75-55	30-75	50-0
GC523-89	157-178 (71.2)	14.7(14.39)					≥120	95-60	20-95	65-0
GC523-91	157-178 (219.2)	14.7 (12.11)					85-95	135-55	30-75	80-10
GC523-99	157-178 (66.4)	14.7 (13.92)					≥105	85-50	30-65	45-0
GC523-102	157-178 (68.0)	14.7 (14.14)					≥110	80-55	30-65	45-0
GC523-105	800-1100 (60.6)	14.7 (12.60)					115-125	90-60	55-75	40-0
GC523-106	178-208 (275.7)	14.7 (10.85)					85-90	80-20	25-65	20-0
GC523-108	208-290 (179.6)	14.7 (10.19)					90-100	65-0		
GC523-109	800-1100 (270.9)	14.7 (10.35)					95-100	280-50	55-90	40-0
RD17-41	800 (179.8)	14.7 (11.98)	>100	245-195	80-90	175-60			55-75	30-0
RD17-42	420 (207.9)	14.7 (11.76)	>100	280-225			75-95	225-25	60-80	25-0
RD17-43	800 (213.7)	14.7 (11.89)	>100	280-170			75-90	175-25	40-70	25-0
RD17-44	420 (187.7)	14.7 (11.96)	>100	260-205			70-85	205-30	70-80	30-0
RD17-45	420 (195.1)	14.7 (12.02)	>100	270-225					70-80	30-0
RD17-46	420 (204.1)	14.7 (12.14)	>100	265-225					70-80	35-0
RD17-47	420 (202.9)	14.7 (12.28)	>100	270-220					70-80	45-0
RD17-48	420 (188.6)	14.7 (12.02)	>100	255-200			80-85	100-25	35-65	20-0
Overlap				**245-225 Ma**		**175-100 Ma**		**65-60 Ma**		**20-10 Ma**

Table 2. Summary of palaeotemperatures analysis and Default Thermal History interpretation